1 **Effects of spatially heterogeneous lakeside development on nearshore biotic communities in a large,**

2 **deep, oligotrophic lake (Lake Baikal, Siberia)**

3 Michael F. Meyer[1]*

4 Ted Ozersky[2]

5 Kara H. Woo[3]

6 Kirill Shchapov[2]

7 Aaron W. E. Galloway[4]

8 Julie B. Schram[4]

9 Emma J. Rosi[5]

10 Daniel D. Snow[6]

11 Maxim A. Timofeyev[7]

12 Dmitry Yu. Karnaukhov[7]

13 Matthew R. Brousil[3]

14 Stephanie E. Hampton[3]

15 [1.] School of the Environment, Washington State University, Pullman, WA, USA

16 [2.] Large Lakes Observatory, University of Minnesota - Duluth, Duluth, MN, USA

17 [3.] Center for Environmental Research, Education, and Outreach, Washington State University,

18   Pullman, WA, USA

19 [4.] Oregon Institute of Marine Biology, University of Oregon, Charleston, OR, USA

20 [5.] Cary Institute of Ecosystem Studies, Millbrook, NY, USA

21 [6.] School of Natural Resources, University of Nebraska-Lincoln, Lincoln, NE, USA

22 [7.] Biological Research Institute, Irkutsk State University, Irkutsk, Irkutsk Oblast, Russia

23 *corresponding author: michael.f.meyer@wsu.edu

24 **Running Head:** Baikal littoral foodwebs

25 **Keywords**: sewage, PPCP, food webs, fatty acids, human disturbance

26 **Statement of novelty, significance, and breadth of interest of the science presented in the**

27 **proposed manuscript**

28 We examined food web responses to heterogenous disturbance along the shoreline of

29 oligotrophic Lake Baikal. Using sewage-specific indicators (pharmaceuticals and personal care

30 products) we demonstrated that increased nutrients at three discrete lakeside developments (80-

31 1,963 permanent residents) and the associated increased filamentous benthic algal abundance

32 were consistent with sewage pollution. This is the first study to provide robust evidence that

33 recent benthic algal blooms are caused by sewage. These changes in benthic algae altered

34 resources and nutrition for grazing invertebrates, whose composition differed at disturbed sites.

35 Stable isotope and fatty acid analysis of benthic algae and macroinvertebrates suggested that

36 grazers at sewage disturbed sites compensate for changing resource nutrition through behavior or

37 altered metabolism. This study demonstrates how patchy, low-level eutrophication of

38 oligotrophic systems can cause food webs to respond in less visible ways.

39

40 **Statement indicating why L&O is the best outlet for the work**

41 This study will appeal to L&O readers interested in both basic and applied issues. From a basic

42 ecology perspective, we investigate how bottom-up disturbances can propagate throughout a

43 food web. From an applied perspective, we highlight how our results can inform monitoring

44 programs. Additionally, we use a suite of interdisciplinary techniques in a manner appreciated by

45 limnologists and oceanographers, such that L&O seems like the perfect home for this

46 manuscript.

47

48 **Abstract**

49 Sewage released from lakeside development can reshape ecological communities. In particular,

50 nearshore periphyton can rapidly assimilate sewage-associated nutrients, leading to increases of

51 filamentous algal abundance, thus altering both food abundance and quality for grazers. In Lake

52 Baikal, a large, ultra-oligotrophic, remote lake in Siberia, filamentous algal abundance has

53 increased near lakeside developments, and localized sewage input is the suspected cause. These

54 shifts are of particular interest in Lake Baikal, where endemic littoral biodiversity is high,

55 lakeside settlements are mostly small, tourism is relatively high (~1.2 million visitors annually),

56 and settlements are separated by large tracts of undisturbed shoreline, enabling investigation of

57 heterogeneity and gradients of disturbance. We surveyed sites along 40 km of Baikal's

58 southwestern shore for sewage indicators – pharmaceuticals and personal care products (PPCPs)

59 and microplastics – as well as periphyton and macroinvertebrate abundance and indicators of

60 food web structure (stable isotopes and fatty acids). PPCPs, including caffeine and

61 acetaminophen/paracetamol, were spatially related to lakeside development. As predicted,

62 lakeside development was associated with more filamentous algae and lower abundance of

63 sewage-sensitive mollusks. Periphyton and macroinvertebrate stable isotopes and essential fatty

64 acids suggested that food web structure otherwise remained similar across sites; yet, the

65 invariance of amphipod fatty acid composition, relative to periphyton, suggested that grazers

66 adjust behavior or metabolism to compensate for different periphyton assemblages. Our results

67 demonstrate that even low levels of human disturbance can result in spatial heterogeneity of

68 nearshore ecological responses, with potential for creating less visible effects that propagate

69 through the food web.

70

71

Introduction

72

73 The release of treated and untreated wastewater into aquatic ecosystems is a common human

74 disturbance that can introduce pollutants and reshape aquatic ecological communities (Moore et

75 al. 2003). Nitrogen and phosphorus are among the primary pollutants in wastewater and its

76 associated byproducts (Smith et al. 1999), yet these nutrients can also originate from disparate

77 anthropogenic and natural environmental sources, thereby complicating their use as sewage

78 indicators. For example, agriculture (Powers et al. 2016), watershed processes such as melting

79 permafrost (Turetsky et al. 2000), and changes in terrestrial plant communities (Moran et al.

80 2012) can all increase allochthonous nutrient inputs similar to sewage. Regardless of the

81 nutrients' source, biological processes can further confound sewage detection. Benthic primary

82 producers, especially those in oligotrophic systems, can assimilate nutrients quickly from the

83 water column (e.g., hours), such that elevated nutrient concentrations may not be not observed

84 (Hadwen and Bunn 2005).

85

86 Because nutrients come from numerous non-sewage sources, indicators consistently associated

87 with human activity, such as enhanced $\delta^{15}N$ stable isotope signatures (Costanzo et al. 2001;

88 Camilleri and Ozersky 2019), pharmaceuticals and personal care products (PPCPs) (Rosi-

89 Marshall and Royer 2012; Meyer et al. 2019) and microplastics (Barnes et al. 2009), have

90 garnered increasing attention for their usefulness as sewage indicators. Stable isotopes, such as

91 $\delta^{15}N$, have been frequently used to trace sewage pollution (Gartner et al. 2002), yet their

92 potential to indicate sewage can be obfuscated by complex terrestrial (Craine et al. 2018) and

93 aquatic (Guzzo et al. 2011) processes. PPCP studies from continental (Kolpin et al. 2002;

94 Focazio et al. 2008; Yang et al. 2018) to colloidal pore (Yang et al. 2016) scales, have shown

95 that PPCP concentrations tend to be greatest closer to their source. In addition to identifying

96   areas and periods of sewage pollution, PPCPs have also demonstrated robustness in defining

97   gradients of sewage pollution in river systems, with concentrations being directly proportional to

98   population density and inversely proportional to distance from a densely populated area (Bendz

99   et al. 2005). Similar to PPCPs, microplastics (plastic debris up to 5 mm in size) also have been

100   useful to detect sewage pollution (Li et al. 2018) along gradients of increasing human population

101   density (Klein et al. 2015), although they can sometimes originate from non-sewage sources,

102   such as shoreline debris or fishing nets (Free et al. 2014). In contrast to $\delta^{15}N$ signatures and

103   PPCPs concentrations, microplastics are typically resistant to degradation (Barnes et al. 2009),

104   providing a signal over a longer time frame than many PPCPs and nutrients in sewage. As a

105   result of each pollutant's consistent association with sewage, co-located $\delta^{15}N$, PPCP, and

106   microplastic measurements can be used to infer the spatial extent and timing of sewage pollution

107   in an ecosystem.

108

109   The effects of sewage pollution are frequently first seen in nearshore benthic communities where

110   increased nutrients alter algal species composition, abundance, nutritional quality, as well as

111   food web trophic structure. Increased filamentous algal abundance, for example, has been

112   frequently observed in areas suspected of sewage pollution (Rosenberger et al. 2008; Hampton et

113   al. 2011), likely due to benthic filamentous algae efficiently removing nutrients from the water

114   column (Hadwen and Bunn 2005; Andersson and Brunberg 2006). With a changing resource

115   base, grazing macroinvertebrate communities may likewise shift to include more detritivores or

116   species capable of consuming filamentous algae (Rosenberger et al. 2008). In addition to some

117   grazers' physical difficulty consuming filamentous algae (Mazzella and Russo 1989), there also

118   may be changes in algal nutritional quality, as filamentous algae tend to contain a different

119   mixture of essential fatty acids (EFAs) in comparison to diatoms (Kelly and Scheibling 2012),

120   which dominate periphyton communities in unimpacted ecosystems. In particular, the EFAs

121   18:3ω3 and 18:2ω6 are commonly associated with green filamentous algae (Taipale et al. 2013),

122   whereas 20:5ω3 is more associated with diatoms (Taipale et al. 2013). All EFAs are largely

123   synthesized by primary producers, and each related group produces strongly differentiated

124   multivariate signatures (Taipale et al. 2013; Galloway and Winder 2015). Consumers can acquire

125   fatty acids by grazing (Dalsgaard et al. 2003) or upgrading fatty acids at their own energetic

126   expense (Sargent and Falk-Petersen 1988; Dalsgaard et al. 2003) and often reflect the fatty acid

127   signatures of their diets. Thus, comparing consumer and producer fatty acid compositions can be

128   used to infer how grazing patterns change in response to increasing sewage pollution.

129

130   To investigate lake littoral community and food web responses to sewage pollution, we surveyed

131   40 km of Lake Baikal's shoreline for indicators of sewage pollution and metrics of benthic

132   community composition and structure. Located in Siberia, Lake Baikal is the oldest, most

133   voluminous, and deepest freshwater lake in the world (Hampton et al. 2018), with the majority of

134   Lake Baikal's biodiversity occurring in the littoral zone (Kozhova and Izmest'eva 1998). While

135   Lake Baikal's pelagic zone is generally ultra-oligotrophic (Yoshida et al. 2003; O'Donnell et al.

136   2017), nearshore areas abutting lakeside settlements have shown distinct signs of eutrophication

137   (Timoshkin et al. 2016). Much of Lake Baikal's shoreline lacks human development, and

138   Baikal's watershed is largely roadless and unpopulated (Moore et al. 2009). Despite low levels of

139   development, uncharacteristic filamentous algal blooms have been occurring throughout the lake

140   since 2010 (Kravtsova et al. 2014; Timoshkin et al. 2016; Volkova et al. 2018). While increased

141   *Ulothrix* spp. abundance historically occurs in late summer (Kozhov 1963; Kozhova and

142   Izmest'eva 1998), recent observations of *Spirogyra* spp. abundance at unprecedented levels are

143   thought to be associated with increased nearshore nutrient concentrations (Volkova et al. 2018;

144   Ozersky et al. 2018). Inadequate wastewater management in lakeside settlements is likely the

145   main driver of these nearshore algal blooms (Timoshkin et al. 2016, 2018), motivating further

146   research to identify the extent to which sewage is altering nearshore communities

147

148   Given the growing evidence that Baikal's nearshore periphyton communities are responding to

149   sewage inputs, our goal was to understand how littoral benthic community composition and

150   interactions may be changing near areas of sewage pollution. This overarching goal was divided

151   into three specific objectives:

152   1.   identify areas of wastewater pollution using consistent sewage indicators,

153   2.   assess the relationship between sewage indicators and littoral periphyton and

154   macroinvertebrate community composition, and

155   3.   evaluate how food webs may restructure with increasing sewage pollution.

156   We hypothesized that (1) sewage indicators, such as PPCP concentrations, δ^{15}N, and

157   microplastic densities, would increase with increasing population density and proximity of

158   lakeside development; (2) an increasing sewage signal would correlate with increased dominance

159   of filamentous benthic algae; and (3) increasing filamentous algae abundance would result in

160   changes in the abundance of different macroinvertebrate feeding guilds, reflected in community

161   composition and dietary tracers such as carbon and nitrogen stable isotopes and fatty acids.

162

163   **Methods**

164   *Site description*

The vast majority of Lake Baikal's 2,100-km shoreline lacks lakeside development (Moore et al.
2009; Timoshkin et al. 2016). Our study focused on a 40-km section of Baikal's southwestern
shoreline, which included three settlements of different sizes (Figure 1; Figure 2). From 19
through 23 August 2015, we sampled 14 littoral and 3 pelagic locations along our 40-km
transect. Littoral locations were chosen to capture a range of sites with varying degrees of
adjacent shoreline development – from "developed" (along the waterfront of human settlements)
to "undeveloped" (no adjacent human settlements and complete forest cover; Figure 1; Figure 2;
Table 1). Pelagic sites were located 2 to 5 km offshore from each of the developed sites in water
depths of 900 to 1300 m (Figure 1; Table 1). All littoral sites were sampled at approximately the
same depth (~1.25 m) at a distance of 8.90 to 20.75 m from shore (Table 1). At each site, air
temperature was measured with a mercury thermometer, and photographs were taken of the
substrate and the shoreline.

Three discrete lakeside settlements were located along our 40-km transect. The largest,
Listvyanka, is primarily a tourist town of approximately 2000 permanent residents, although
tourism can contribute significantly to the town's population with approximately 1.2 million
annual visitors (Interfax-Tourism 2018). The other two settlements are the villages Bolshie Koty
and Bolshoe Goloustnoe, which have approximately 80 and 600 permanent residents,
respectively. Bolshie Koty is home to two field research stations and several small tourist
accommodations. Bolshoe Goloustnoe has several hotels and tourist camps. Although Bolshie
Koty and Bolshoe Goloustnoe are built along small streams that empty into Baikal, there are no
upstream developed sites, meaning that any observed sewage indicators in Baikal most likely
originated either from Bolshie Koty or Bolshoe Goloustnoe.

188

Inverse distance weighted (IDW) population calculation

190   We recognized that sewage indicator concentrations at each sampling location may be related to

191   a sampling location's spatial position relative to both the size and proximity of neighboring

192   developed sites. Therefore, we created the inverse distance weighted (IDW) population metric to

193   compress, into a single metric, information about human population size, density, and location

194   along the shoreline as well as distance between developed sites and sampling locations. The

195   IDW metric reflects the idea that sewage pollution should be positively related to increasing

196   human density and inversely related with distance from densely populated areas (sensu Bendz et

197   al., 2005). Additionally, Timoshkin et al. (2018) noted that sewage enters Baikal's nearshore

198   largely through groundwater, implying that locations with more directly adjacent shoreline

199   development should experience higher sewage concentrations in the lake. Acknowledging that

200   nearshore PPCP concentrations were likely positively proportional to a developed location's

201   shoreline length, we scaled a developed site's population density by its shoreline length. This

202   scaling represents population density that directly interfaces with the lake, thereby capturing the

203   idea that sewage-associated pollutants, such as PPCPs (Karnjanapiboonwong et al. 2010) and

204   nutrients (de Vries 1972), contributed away from the shoreline can be removed via the soil

205   matrix en route to the lake.

206

207   Our calculation of IDW population was done in five steps. First, we traced polygons and

208   shorelines from satellite imagery for each developed site in Google Earth. Polygons were traced

209   for the entire area of visible development (Figure 2). Similarly, shoreline traces only reflected

210   shoreline length for which there was visible development (Figure 2). Second, polygon and line

211   geometries were downloaded from Google Earth as a .kml file. Third, the .kml file was imported

212   into the R statistical environment (R Core Team 2019) where, using the sf package (Pebesma,

213   2018), we calculated shoreline length, polygon area, and centroid location for each developed

214   site. Fourth, we joined point locations of each sampling site with the spatial polygons to calculate

215   the distance from each sampling location to each developed site's centroid. Fifth, we calculated

216   IDW population for each sampling location, using formula (1)

217   (1) $Ij = \dfrac{\frac{P_{LI}}{A_{LI}}*L_{LI}}{D_{j,LI}} + \dfrac{\frac{P_{BK}}{A_{BK}}*L_{BK}}{D_{j,BK}} + \dfrac{\frac{P_{BGO}}{A_{BGO}}*L_{BGO}}{D_{j,BGO}}$

218   where I is the IDW population at sampling location j, P is the population at each of the three

219   developed sites Listvyanka (LI), Bolshie Koty (BK), Bolshoe Goloustnoe (BGO), A is the area of

220   a developed site in km^2, L is the shoreline length at a developed site in km, and D is the distance

221   from sampling site j to each developed site's centroid in km. This formulation implies that all

222   sampling locations are influenced by all three developed sites. Thus, the influence of an

223   individual developed site on each sampling location is positively influenced by the size and

224   spatial density of the population and its orientation toward the shoreline, and inversely

225   proportional to a sampling location's distance from each of the three developed sites.

226

227   *Water samples*

228   At both pelagic and littoral sites, water samples were collected for nutrient, chlorophyll,

229   microplastic, and PPCP analysis. Samples were collected by hand from 0.75 m depth for each

230   littoral site and with a bucket from aboard the Irkutsk State University "Kozhov" research vessel

231   for pelagic sites. Each water sample collection procedure is described below.

232

233   *Nutrients*

234   Water samples for nutrient analyses were collected in 150 mL glass jars that had been washed

235   with phosphate-free soap and rinsed three times with water from the sampling location. Samples

236   were collected in duplicates and immediately frozen at -20°C until processing at the A.P.

237   Vinogradov Institute of Geochemistry (Siberian Branch of the Russian Academy of Sciences,

238   Irkutsk). Samples were not filtered prior to freezing, meaning that nitrogen and ammonium

239   concentrations may potentially include intracellular nitrogen and overestimate nitrogenous forms

240   in the water column.

241

242   For each water sample, nitrate, ammonium, and total phosphorus concentrations were measured.

243   For ammonium (2016a) and nitrate (2017) concentrations, samples were analyzed with a

244   spectrophotometer following the addition of Nessler's reagent and disulfuric acid respectively.

245   Total phosphorus concentration was measured with a spectrophotometer following the addition

246   of persulfate (2016b). Concentrations are reported in mg/L.

247

248   *Chlorophyll a*

249   Water samples were collected in 1.5 L plastic bottles from a depth of approximately 0.75 m.

250   Within 12 h of collection, three subsamples (up to 150 mL each) were filtered through 25-mm

251   diameter, 0.2 μm pore size nitrocellulose filters. Filters were then placed in a 35-mm petri dish

252   and frozen in the dark until processing.

253

254   Chlorophyll samples were processed in a manner similar to that of Parsons and Strickland (1963)

255   and Lorenzen (1967). Nitrocellulose filters were ground in 90% acetone, in which chlorophyll

256   extraction was allowed to proceed overnight. Samples were then centrifuged for 15-20 minutes.

257   After centrifugation, absorbance of the chlorophyll extract was measured in a spectrophotometer

258   at 630, 645, 665, and 750 nm. Concentrations were calculated using the formula: $C =$

259   $11.64(A_{665} - A_{750}) - 2.16(A_{645} - A_{750}) - 0.1(A_{630} - A_{750}) / (V_2/V_1)$; where A is the

260   absorbance value of a particular wavelength, V_1 is the volume of the filtered water, and V_2 is the

261   volume of extract. Concentrations are reported as mg/L.

262

263   *PPCPs*

264   Water samples for PPCP analysis were collected in 250 mL amber glass bottles that were rinsed

265   with either methanol or acetone and then three times with sample water prior to collections.

266   Following collection, samples were refrigerated and kept in the dark until solid phase extraction

267   (SPE).

268

269   Within 12 h of collection, samples were filtered directly from the amber glass bottle using an in-

270   line Teflon filter holder with glass microfiber GMF (1.0 μm pore size, WhatmanGrad 934-AH)

271   in tandem with a solid phase extraction (SPE) cartridge (200 mg HLB, Waters Corporation,

272   Milford, MA) connected to a 1-liter vacuum flask. Lab personnel wore gloves and face masks to

273   minimize contamination. Prior to filtration, SPE cartridges were primed with at least 5 mL of

274   either methanol or acetone and then washed with at least 5 mL of sample water. Rate of

275   extraction was maintained at approximately 1 drop per second. Extraction proceeded until water

276   could no longer pass through the SPE cartridge or until all collected water was filtered.

277   Cartridges were stored in Whirlpacks at -20°C until analysis for 18 PPCP residues using liquid

278   chromatography tandem mass spectrometry (LC-MS-MS) following methods of Lee et al. (2016)

279   and D'Alessio et al (2018). Concentrations are reported in μg/L.

280

Microplastics

At each location, samples were collected in triplicate using 1.5 L clear plastic bottles that were washed thoroughly with sample water before each collection. Samples were collected by hand for each littoral site and with a metal bucket from aboard the ship for pelagic sites.

For processing, each sample was vacuum filtered on to a 47-mm diameter GF/F filter. During filtration, aluminum foil was used to cover the filtration funnel to prevent contamination from airborne microplastic particles. After filtration, filters were dried under vacuum pressure and then stored in 50-mm petri dishes. Following filtration of all three replicates, the filtrate was collected and then re-filtered through a GF/F filter as a control for contamination from the plastic vacuum funnel or potentially airborne microplastics.

Microplastic counting involved visual inspection of the entire GF/F in a similar manner to methods described in Hanvey et al. (2017). Visual enumeration was conducted under a stereo microscope with ~100x magnification, and microplastics were classified into one of three categories: fibers, fragments, or beads. For all categories, plastics were defined as observed objects with apparent artificial colors, so as to not enumerate plastics potentially contributed from the sampling bottle itself. Fibers were defined as smooth, long plastics with consistent diameters. Fragments were defined as plastics with irregularly sharp or jagged edges. Beads were defined as spherical plastics. Although we did not measure microplastic size, this technique likely allowed us to reliably quantify microplastics as small as ~300 μm (Hanvey et al. 2017). During enumeration, GF/Fs remained covered in the petri dish to minimize potential for

303   contamination from the air. Following enumeration of both experimental and control samples,

304   fibers, fragments, and beads enumerated in the controls were subtracted from the experimental

305   microplastic densities for each plastic type and from each replicate. One location (BK-1) had two

306   control replicates, which were averaged for each plastic type and then subtracted from the

307   experimental samples. Results are reported as the average number of microplastics/L.

308

309   *Benthic biological samples*

310   At each littoral site, periphyton and macroinvertebrates were collected for relative abundance

311   estimates and food web analysis by wading and snorkeling.

312

313   *Benthic algal collection*

314   At each littoral site, we haphazardly selected three rocks representative of local substrate. A

315   plastic stencil was used to define a surface area of each rock from which we scraped a

316   standardized 14.5 cm^2 patch of periphyton. Samples were preserved with Lugol's solution and

317   stored in plastic scintillation vials. Additional periphyton was collected in composite from each

318   site for fatty acid and stable isotope analysis.

319

320   Periphyton taxonomic identification and enumeration was performed by subsampling 10 μL

321   aliquots from each preserved sample. For all 10 μL aliquots, cells, filaments, and colonies were

322   counted, for the entire subsample, until at least 300 cells were identified for a given sampling

323   replicate. If the first aliquot contained less than 300 cells, we counted additional subsamples until

324   we reached at least 300 cells in total. In instances when 300 cells were counted before finishing a

325   subsample, we still counted the entire aliquot. Taxa were classified into broad categories

326   consistent with Baikal algal taxonomy (Izhboldina 2007), using coarse groupings to capture

327   general patterns in relative algal abundance. As a result, algal groups consisted of diatoms,

328   *Ulothrix*, *Spirogyra*, and the green algal Order Tetrasporales.

329

330   *Benthic invertebrate collection*

331   At each littoral site, three kick-net samples were collected for assessment of benthic community

332   composition and abundance. Using a D-net, we collected macroinvertebrates by flipping over 1-3

333   rocks, and then sweeping five times in a left-to-right motion across approximately 1 m. After the

334   series of sweeps, the catch was rinsed into a plastic bucket. For each replicate, bucket contents

335   were concentrated using a 64-μm mesh and placed in glass jars with 40% ethanol (vodka; the

336   only preservative available to us at the time) for preservation and refrigerated at 4°C aboard the

337   research vessel. The 40% ethanol preservative was replaced with ~80% ethanol upon return to

338   the lab within 24 to 48 hours, and samples were stored at ~4°C.

339

340   Separate collections were conducted for invertebrate fatty acid and stable isotope analyses.

341   Invertebrates were collected using a D-net in a similar fashion as the community enumeration.

342   Additional invertebrates were also collected by hand. Collected organisms were then live-sorted,

343   identified to species, and frozen at -20°C at the field station. The samples were later transferred

344   to the lab in the US via a Dewar flask with dry ice.

345

346   Invertebrate taxonomic identification and enumeration were performed under a stereo

347   microscope. All invertebrates were identified to species with the exception of juveniles

348   (Takhteev and Didorenko (2015) for amphipods; Sitnikova (2012) for mollusks; Table 2). All

349   samples contained oligochaetes and polychaetes, but due to poor preservation, these taxa were

350   not counted. Six samples of the 42 collected were not well-preserved and were excluded from

351   further analyses, in order to reduce errors in identification. KD-1 and LI-1 were the only sites

352   with 1 sample counted. BK-2 and KD-2 each had two samples counted.

353

354   *Food web characterization*

355   To characterize littoral food webs, we analyzed carbon and nitrogen stables isotopes as well as

356   fatty acid profiles for periphyton and macroinvertebrates. Prior to isotopic and fatty acid

357   analysis, periphyton and macroinvertebrate samples were lyophilized for ~24 hours,

358   homogenized to powder, and then weighed.

359

360   *Stable isotope analysis*

361   Measurements of $\delta^{15}N$ and $\delta^{13}C$ were performed on an elemental analyzer-isotope ratio mass

362   spectrometer (EA-IRMS; Finnigan DELTAplus XP, Thermo Scientific) at the Large Lakes

363   Observatory, University of Minnesota Duluth. The EA-IRMS was calibrated against certified

364   reference materials including L-glutamic acid (NIST SRM 8574), low organic soil and sorghum

365   flour (standards B-2153 and B-2159 from Elemental Micro-analysis Ltd., Okehampton, UK) and

366   in-house standards (acetanilide and caffeine). Replicate analyses of external standards showed a

367   mean standard deviation of 0.06 ‰ and 0.09 ‰, for $\delta^{13}C$ and $\delta^{15}N$, respectively.

368

369   *Fatty acid analysis*

370   Following freeze-drying, samples were transferred to 10 mL glass centrifuge vials, and 2 mL of

371   100% chloroform was added to each under nitrogen gas. Samples remained in chloroform

372   overnight at -80°C. Fatty acid extractions generally involved three phases: (1) 100% chloroform

373   extraction, (2) chloroform-methanol extraction, and (3) fatty acid methylation. Fatty acid

374   extraction methods were adapted from Schram et al. (2018).

375

376   After overnight chloroform extraction, samples underwent a chloroform-methanol extraction

377   three times. To each sample, we added 1 mL cooled 100% methanol, 1 mL chloroform:methanol

378   solution (2:1), and 0.8 mL 0.9% NaCl solution. Samples were inverted three times and sonicated

379   on ice for 10 minutes. Next, samples were vortexed for 1 minute, and centrifuged for 5 minutes

380   (3,000 rpm) at 4°C. Using a double pipette technique, the lower organic layer was removed and

381   kept under nitrogen. After the third extraction, samples were evaporated under nitrogen flow, and

382   resuspended in 1.5 mL chloroform and stored at -20°C overnight.

383

384   Once resuspended in chloroform, 1 mL of chloroform extract was transferred to a glass

385   centrifuge tube with a glass syringe as well as an internal standard of 4 μL of 19-carbon fatty

386   acid. Samples were then evaporated under nitrogen, and then 1 mL of toluene and 2 mL of 1%

387   sulfuric acid-methanol was added. The vial was closed under nitrogen gas and then incubated in

388   50°C water bath for 16 hours. After incubation, samples were removed from the bath, allowed to

389   reach room temperature and stored on ice. Next, we performed a potassium carbonate-hexane

390   extraction twice. To each sample, we added 2 mL of 2% potassium bicarbonate and 5 mL of

391   100% hexane, inverting the capped vial so as to mix the solution. Samples were centrifuged for 3

392   minutes (1,500 rpm) at 4°C. The upper hexane layer was then removed and placed in a vial to

393   evaporate under nitrogen flow. Once almost evaporated, 1 mL of 100% hexane was added and

394   stored in a glass amber autosampler vial for GC/MS quantification. GC/MS quantification was

395   performed with a Shimadzu QP2020 GC/MS following Schram et al. (2018).

396

397 *Statistical analyses*

398 Total phosphorus, nitrate, ammonium, microplastic abundance and density, total PPCP

399 concentration, and $\delta^{15}N$ values in macroinvertebrate tissues were log-transformed and regressed

400 against log-transformed IDW population using a linear model. Analytically, log-transforming

401 made sites comparable, as values spanned three orders of magnitude. Physically, we assumed

402 that sewage indicators were likely subject to exponential processes (e.g., mixing, diffusion), and

403 log-transforming the data should linearize the relationships between predictor and response

404 variables. Residuals were assessed for normality and homogeneity of variance.

405

406 To assess if benthic community composition was associated with increasing sewage indicators,

407 periphyton and macroinvertebrate abundance data were each analyzed with a consistent

408 multivariate workflow. First, replicates were averaged, and taxonomic groups representing less

409 than 1% of the inter-site community were removed from analysis, in order to reduce the

410 influence of rare species on results. Second, community compositions for both periphyton and

411 macroinvertebrates were visualized using non-metric multidimensional scaling (NMDS) with a

412 Bray-Curtis similarity metric. Periphyton community compositions were calculated as relative

413 proportions, whereas invertebrate abundances were grouped at the genus-level and then square-

414 root transformed to minimize influence of more abundant taxa. Visual inspection of the NMDS

415 plot suggested that sites generally tended to separate by increasing PPCP concentrations and

416 IDW population (see Table 2). To test whether sites' benthic communities significantly differed

417 with increasing PPCP concentration and IDW population, we first used k-mediods, also known

418 as Partitioning Around the Mediods (PAM; Kaufman and Rousseeuw 2005), clustering to

419 identify an optimal number of groupings (Figure S1). For this process, we iterated through

420 multiple numbers of clusters (i.e., 1 to 10) and calculated the within-group-sum-of-squares ($_{WSS}$)

421 and average silhouette width. We identified the optimal number of groups when wss decreased

422 most markedly and when silhouette width was greatest (i.e., the elbow method) (Johnson and

423 Wichern 2007). To confirm the optimal number as determined by non-hierarchical PAM

424 clustering, we also used Weighted Pair-Group Centroid Clustering (WPGMC) as a hierarchical

425 approach (Sneath and Sokal 1973), which corrects for clusters that may not be strongly

426 discriminated regardless of how many samples are assigned to a given cluster (Legendre and

427 Legendre 2012). We then performed two permutational multivariate analyses of variance

428 (PERMANOVA; Anderson 2001) with 999 permutations: the first where community

429 compositions were responses to the groups identified through clustering and the second where

430 community compositions were responses to the continuous IDW population. Unlike traditional

431 multivariate analyses of variance (MANOVA), PERMANOVA does not require assumptions of

432 multivariate normality (Anderson 2001). When significant differences were identified, post-hoc

433 SIMPER analysis (Clarke 1993) was performed following the PERMANOVA to identify which

434 taxonomic groups contributed to 85% of the cumulative variance that most influenced site

435 separation.

436

437 To assess whether benthic food webs restructured with increasing sewage indicator

438 concentrations, fatty acid data were analyzed in a manner similar to periphyton and

439 macroinvertebrate abundance data. First, species' fatty acid profiles were visualized by

440 performing NMDS with Bray-Curtis similarity for all organisms' relative fatty acid abundance

441 (Figure S2). This technique broadly demonstrated that, as expected, interspecific variation in

442   fatty acid composition was greater than intraspecific variation. The same pattern was observed

443   for all fatty acids quantified as well as solely essential fatty acids (EFAs; Figure S2). Together,

444   these NMDS plots suggested that periphyton fatty acids at sites differentiated based on sewage

445   indicator concentrations, which was likely a reflection of differences in periphyton community

446   composition (Taipale et al. 2013). Among all taxa and sites, 18:3ω3, 18:1ω9, and 20:5ω3 had the

447   highest coefficients of variation, enabling comparisons between sites. These fatty acids tend to

448   be associated with filamentous green algae (i.e., 18:3ω3 and 18:1ω9) and diatoms (i.e., 20:5ω3).

449   To increase the robustness of our analysis, we expanded our approach to include major fatty

450   acids within each taxonomic group, including 18:2ω6 (abundant in green algae); 16:1ω7 and

451   14:0 (abundant in diatoms); and 16:0 (abundant in both green algae and diatoms) (Taipale et al.

452   2013). To evaluate how relative fatty acid abundance may relate to sewage pollution, we

453   assessed patterns among these seven fatty acids with both multivariate and univariate

454   approaches. Within a multivariate framework, we created two NMDS plots with Bray-Curtis

455   similarity, one just with primary producer (Figure S5) and the other with macroinvertebrate

456   (Figure S6) fatty acid profiles. Because multivariate patterns suggested fatty acid profiles may

457   relate to sewage pollution, we regressed a filamentous:diatom fatty acid ratio (Equation 2)

458     $$(2) \quad \frac{18\!:\!3\omega3\% + 18\!:\!1\omega9\% + 18\!:\!2\omega6\% + 16\!:\!0\%}{20\!:\!5\omega3\% + 16\!:\!1\omega7\% + 16\!:\!0\% + 14\!:\!0\%}$$

459   against log-transformed PPCP concentrations using a linear model. Additionally, we evaluated

460   how three essential fatty acids (18:3ω3, 18:2ω6, and 20:5ω3), lipids thought to accumulate in

461   biological systems, may differ in abundance across the sewage gradient. Therefore, we similarly

462   regressed the ratio of $\frac{18\!:\!3\omega3\% + 18\!:\!2\omega6\%}{20\!:\!5\omega3\%}$ against log-transformed PPCP concentrations using a

463   linear model.

464

465   All analyses were conducted in the R statistical environment (R Core Team 2019), using the

466   tidyverse (Wickham et al. 2019), factoextra (Kassambara and Mundt 2019), cluster (Maechler et

467   al. 2019), pvclust (Suzuki et al. 2019), ggrepel (Slowikowski 2019), viridis (Garnier 2018), fs

468   (Hester and Wickham 2019), spdplyr (Sumner 2019), janitor (Firke 2020), sf (Pebesma 2018),

469   ggpubr (Kassambara 2019), ggtext (Wilke 2020), OpenStreetMap (Fellows and Stotz 2019),

470   cowplot (Wilke 2019), and vegan (Oksanen et al. 2019) packages. All data, including .kml files

471   used to calculate IDW metric, are publicly available from the Environmental Data Initiative

472   repository (Meyer et al. 2020), and all R scripts are available from the GitHub repository of this

473   project's Open Science Framework account (Meyer et al. 2015).

474

475   **Results**

476   *Water samples*

477   Nearshore water nitrate ($R^2 = 0.01$, $p = 0.68$), ammonium ($R^2 = 0.17$, $p = 0.11$), total phosphorus

478   ($R^2 = 0.14$, $p = 0.14$), and chlorophyll a ($R^2 = 0.11$, $p = 0.20$) concentrations were not

479   significantly correlated with IDW population (Figure 3). Total PPCP ($R^2 = 0.26$, $p = 0.04$)

480   concentrations were significantly related with IDW population (Figure 3). In the littoral zone,

481   PPCPs detected included caffeine, 1,7-dimethylxanthine/paraxanthine (main human metabolite

482   of caffeine), cotinine (main human metabolite of nicotine), and acetaminophen/paracetamol

483   (Table 3). Other PPCPs, including carbamazepine, diphenhydramine, thiabendazole,

484   amphetamine, methamphetamine, MDA, MDMA, morphine, phenazone, sulfachloropyridazine,

485   sulfamethazine, sulfadimethoxine, sulfamethazole, trimethoprim, and cimetidine, were not

486   detected.

487

488   Microplastics were detected in samples from both littoral and pelagic sites. Bead microplastics

489   were only detected near Listvyanka. Fibers (mean = 0.85 microplastics/L, std dev = 1.21

490   microplastics/L) and fragments (mean = 0.83 microplastics/L, std dev = 1.35 microplastics/L)

491   were the most abundant types of microplastics across all sites, whereas beads were relatively rare

492   (mean = 0.08 microplastics/L, std dev = 0.31 microplastics/L). Total microplastic densities were

493   not significantly correlated with IDW population (R^2 = 0.01, p = 0.65; Figure 3), although more

494   types of microplastics were generally observed near areas with higher IDW population values,

495   such as Listvyanka.

496

497   *Benthic biological samples*

498   *Periphyton*

499   Major taxonomic groupings of periphyton consisted of diatoms, *Tetrasporales* spp., *Spirogyra*

500   spp., and *Ulothrix* spp. K-mediods (Figures S1a; S2a) and WPGMC (Figure S3a) cluster

501   analyses of periphyton abundance demonstrated two groupings capture most variance, and visual

502   inspection of relative periphyton community abundance NMDS suggested groupings were

503   related to IDW population values (Figure 4). PERMANOVA results demonstrated that

504   periphyton communities were significantly different based on IDW population groupings (R^2 =

505   0.52, p = 0.001) and the continuous IDW population (R^2 = 0.43, p = 0.001). Post-hoc SIMPER

506   results suggested that these differences were primarily associated with sites that had higher

507   *Ulothrix* spp. and *Spirogyra* spp. relative abundance. Additionally, sites with high IDW

508   populations had lower diatom relative abundance in comparison to sites with low and moderate

509   IDW populations.

510

511   *Macroinvertebrates*

512   Taxonomic groupings included five amphipod genera: *Eulimnogammarus*, *Poekilogammarus*,

513   *Cryptoropus*, *Brandtia* and *Pallasea*; six mollusk families: Planorbidae, Valvatidae, Baicaliidae,

514   Benedictidae, Acroloxidae, and Maackia; flatworms; caddisflies; and leeches (summarized in

515   Table S1). K-mediod cluster analysis of macroinvertebrate community composition suggested 2

516   or 3 major groupings would capture most variance (Figure S1b; S2b), whereas WPGMC

517   analyses suggested 2 groupings would enable all sites except for one to be assigned a cluster

518   (S3b). Because both forms of hierarchical and non-hierarchical clustering suggested two

519   groupings as optimal, we proceeded using two groupings. Visual inspection of NMDS suggested

520   clusters were related to IDW population (Figure 5). PERMANOVA results supported the

521   hypothesis that macroinvertebrate communities significantly differed both among our IDW

522   population groupings ($R^2 = 0.19$, $p = 0.02$) and along our continuous gradient of increasing IDW

523   population ($R^2 = 0.19$, $p = 0.02$). Post-hoc SIMPER analyses suggested that *Poekilogammarus*,

524   *Eulimnogammarus*, Valvatidae, Caddisflies, *Brandtia*, Baicaliidae, Planorbidae, *Cryptoropus*,

525   and flatworms contributed the greatest differences between high and moderate/low IDW

526   population groupings (see Table 2).

527

528   *Food web characterization: stable isotopes and fatty acids*

529   Among periphyton and amphipod samples, $\delta^{13}C$ values ranged from -19.5 to -9.5 ‰ (Figure 6).

530   Among periphyton samples, $\delta^{15}N$ values ranged from 0.77 to 3.76 ‰, whereas amphipod $\delta^{15}N$

531   values ranged from 6.42 to 7.92 ‰.

532

533   For grazers, δ^{15}N significantly increased with IDW population (p = 0.01; Figure 3, Figure 6).

534   Periphyton δ^{15}N signatures did not significantly increase with IDW population (p = 0.27). In

535   contrast, δ^{13}C concentrations were not related with IDW population for either periphyton or

536   macroinvertebrates.

537

538   With respect to fatty acids, macroinvertebrates tended to be characterized by mono-unsaturated

539   fatty acids (MUFAs) and long-chain (i.e. $\geq$ 20-Carbons) polyunsaturated fatty acids (LCPUFAs),

540   whereas periphyton tended to be characterized by short-chain (i.e., 16- and 18-Carbons)

541   polyunsaturated fatty acids (SCPUFAs) (Table 3). When comparing proportions within taxa

542   across the sewage gradient, periphyton SCPUFA proportion tended to increase (Figure S4) and

543   periphyton SAFA proportions generally decreased. In contrast, benthic macroinvertebrate fatty

544   acid class proportions tended to remain consistent across the entire gradient (Figure S4).

545

546   For both periphyton and grazers, our analyses focused mainly on the fatty acids consistently

547   associated with filamentous green algae (i.e., 18:3ω3, 18:1ω9, 18:2ω6, and 16:0) as well as

548   diatoms (i.e., 20:5ω3, 16:1ω7, 14:0, and 16:0). For periphyton, the ratio of green

549   filamentous:diatom-associated fatty acids significantly increased with an increasing PPCP

550   concentration (R^2 = 0.62; p = 0.04, Figure 7; S5) but not with an increasing IDW population (p =

551   0.08). Amphipod fatty acid ratios were not significantly related with either increasing IDW

552   population or increasing PPCP concentrations (Figure 7; S6). When focusing solely on the

553   essential fatty acids 18:3ω3, 18:2ω6, and 20:5ω3, the same pattern was observed in both

554   periphyton (R^2 = 0.73; p = 0.02) and amphipods (Figure 7).

555

Discussion

Our combined results corroborate previous findings (e.g., Timoshkin et al., 2016; 2018) that sewage pollution is entering Lake Baikal's nearshore area and likely is responsible for changes in nearshore benthic communities. Unlike previous studies, we were able to incorporate highly specific indicators of sewage pollution and food web structure to offer direct, quantitative relationships between human development and ecological responses.

Relating human settlements to sewage indicator concentrations

In agreement with our expectations, some sewage pollution indicators in the nearshore of Lake Baikal were associated with size of and distance from human settlements. Total PPCP, macroinvertebrate $\delta^{15}N$, and, to some degree, total phosphorus concentrations increased with IDW population. These sewage gradients created by highly localized settlements are noteworthy considering that Baikal's shoreline, including our study area, is largely free of lakeside development (Moore et al. 2009). Furthermore, the use of sewage-associated indicators, such as PPCPs and $\delta^{15}N$, proved necessary for defining sewage gradients. The use of nutrients as indicators alone would not reveal sewage pollution gradients, since nutrients were not strongly correlated with IDW population and could come from diverse sources. For example, melting permafrost in Lake Baikal's watershed (Anisimov and Reneva 2006) and the Selenga River basin (Tornqvist et al. 2014) as well as climate-driven changes in mixing processes (Swann et al. 2020) have the potential to contribute substantial nutrient loadings to the nearshore. While nutrients also could be contributed by agriculture (Powers et al. 2016), atmospheric deposition (Galloway et al. 2004; Monteith et al. 2007; Stoddard et al. 2016), and changing terrestrial plant communities (Moran et al. 2012), these are not currently known to be major sources of elevated

579 nutrients in the Baikal watershed, relative to sewage (Timoshkin et al., 2016, Timoshkin et al.,

580 2018) and permafrost melt (Anisimov & Reneva, 2006).

581

582 This is the first known study to detect PPCPs in Lake Baikal, a voluminous lake in a largely

583 unpopulated watershed. We detected PPCPs nearshore but not at our three offshore sites,

584 suggesting that sewage inputs in Baikal become diluted as pollutants move out of the nearshore

585 area. More generally, these results are important for lake monitoring, as PPCPs are robust

586 indicators of sewage pollution. Beyond Lake Baikal, these data are important for understanding

587 PPCPs' prevalence in lakes, as lakes have remained less represented in the PPCP literature in

588 comparison to lotic and subsurface systems (Meyer et al. 2019). This literature imbalance creates

589 opportunities to assess how PPCPs, and sewage pollution more broadly, may lead to differing

590 ecological responses in lotic and lentic systems. As lakes tend to have longer hydraulic residence

591 times relative to rivers and streams, pollutants may be more prone to accumulate (Yang et al.

592 2018; Meyer et al. 2019). In the case of our data, comparing contemporaneous littoral and

593 pelagic PPCP concentrations revealed littoral-pelagic sewage gradients, as PPCPs were

594 degraded, metabolized or accumulated by biota, preserved within sediments, or diluted to

595 undetectable concentrations. In the context of the entire lake, analyses of sediments have shown

596 how PPCPs can remain within lake systems for decades, thereby enabling researchers to

597 reconstruct histories of wastewater pollution in a system (Czekalski et al. 2015; Yang et al.

598 2018).

599

600 Investigating PPCP concentrations across limnic environments could also establish how

601 ecological communities respond differently not only to sewage but also to the PPCPs themselves.

602   While we focus on PPCPs as indicators of sewage, previous studies have shown that PPCPs,

603   even at concentrations we observed in Lake Baikal, can elicit biological responses from

604   physiological (e.g., del Rey et al. 2011; Feijão et al. 2020) and behavioral (e.g., Brodin et al.

605   2013; Dzieweczynski et al. 2016) levels to food webs (e.g., Lagesson et al. 2016; Richmond et

606   al. 2018) and ecosystems (e.g., Rosi-Marshall et al. 2013; Richmond et al. 2019; Robson et al.

607   2020). Although our study was not designed to evaluate the ecotoxicological effects of PPCPs

608   themselves, future studies could potentially address effects of PPCPs on nearshore Baikal biota

609   by using *in situ* sewage gradients as a guide.

610

611   In contrast to PPCP concentrations and $\delta^{15}N$ values, microplastics were not associated with IDW

612   population and may be poor proxies for sewage pollution in Lake Baikal. Additionally,

613   microplastics may originate from non-sewage sources, such as agriculture (Steinmetz et al. 2016)

614   and fish nets (Eerkes-Medrano et al. 2015). Because of their long degradation time (Brandon et

615   al. 2016), microplastics can indicate accumulated pollution, which likely enables wider

616   distribution from nearshore inputs to the offshore (Fischer et al. 2016; Hendrickson et al. 2018).

617   Unlike microplastic concentrations identified in Lake Hovsgol (Free et al. 2014), Lake Superior

618   (Hendrickson et al. 2018), or Lake Erie (Eriksen et al. 2013), microplastic concentrations in

619   Baikal, as quantified by our methods, may be poor proxies for capturing pollution from

620   seasonally varying human populations. It is worth noting that since the time of our field

621   sampling, evidence has accumulated that our methods likely dramatically underestimated

622   microplastic abundance (Wang and Wang 2018; Brandon et al. 2020), and there is potential for

623   the microplastics themselves to cause deleterious ecological responses. While we focus here on

624   microplastics as an indicator of sewage pollution, microplastics are increasingly shown to disrupt

625   food web dynamics by altering grazing patterns (Green 2016) and providing carbon substrate for

626   microbial growth (Romera-Castillo et al. 2018). Recent investigations of microplastics in Lake

627   Baikal near Bolshie Koty (BK) used analogous methods and measured similarly low

628   concentrations (Karnaukhov et al. 2020). When considering Lake Baikal's large volume,

629   Karnaukov et al. (2020) noted that the number of plastic pieces may well exceed those observed

630   in other lakes, such as Lake Hovsgol. Together these growing uncertainties suggest that

631   microplastic pollution in Baikal and elsewhere deserves increased attention.

632

633   *Relating sewage indicators with benthic algal communities*

634   Congruent with our hypotheses, increasing sewage indicators tended to be associated with higher

635   relative abundance of filamentous taxa in periphyton. Previous studies investigating Baikal's

636   periphyton composition noted that areas adjacent to human development often had increased

637   abundance of filamentous algae such as *Ulothrix* and *Spirogyra* (Timoshkin et al. 2016, 2018).

638   Lake Baikal's southwestern shore historically experiences short *Ulothrix* blooms in late August

639   (Kozhov 1963), potentially confounding sewage signals with an annually occurring

640   phenomenon. Our data are consistent with the results of Timoshkin et al. (2016) and show that

641   relative abundance of filamentous algae is greatest near areas of higher lakeside development.

642

643   While community composition shifted with increasing sewage indicator concentrations,

644   periphyton δ^{15}N values did not differ along our transect. Previous studies in marine (Gartner et

645   al. 2002; Savage and Elmgren 2004; Risk et al. 2009) and freshwater (Wayland and Hobson

646   2001; Camilleri and Ozersky 2019) systems have highlighted how sewage-associated δ^{15}N can

647   increase in algal samples and even throughout the food web. Like PPCPs in our study, δ^{15}N

648   values are often most enriched near the source of sewage pollution and can decrease over several

649   kilometers (Savage and Elmgren 2004), with concentrations varying based on species-specific

650   uptake rates and advective, dispersive, and diffusive transport (Gartner et al. 2002). While

651   previous studies using $\delta^{15}N$ signatures in macroalgae and vascular macrophytes have

652   successfully tracked sewage gradients (Cole et al. 2004), periphyton $\delta^{15}N$ as a sewage indicator

653   potentially can be confounded by terrestrial $\delta^{15}N$ contributions such as through agricultural

654   runoff (Chang et al. 2012). In our study, periphyton $\delta^{15}N$ signatures may be explained by

655   periphyton's typically high cell turnover rates (e.g., days; Swamikannu and Hoagland 1989)

656   dampening isotopic patterns, $\delta^{15}N$-accumulating algal taxa being grazed more readily by

657   macroinvertebrates (Rosenberger et al. 2008), or co-limitation dynamics between ammonium and

658   nitrate (York et al. 2007; Piñón-Gimate et al. 2009).

659

660   Fatty acid analyses suggested that changes in periphyton community composition altered the

661   nutritional quality of periphyton across the pollution gradient. Periphyton fatty acid profiles from

662   sites with higher sewage pollution had higher levels of 18:3ω3, 18:1ω9, 18:2ω6, and 16:0

663   relative to 20:5ω3, 16:1ω7, 16:0, and 14:0 fatty acids. This pattern likely reflects the higher

664   abundance of green algae relative to diatoms (Iverson et al. 2004; Osipova et al. 2009; Taipale et

665   al. 2013; Galloway and Winder 2015; Shishlyannikov et al. 2018), which we observed from our

666   periphyton community composition analysis (Figure 3). Together, our periphyton composition

667   and fatty acid results suggest that Baikal's nearshore periphyton communities near human

668   lakeside developments are more dominated by filamentous green algae, and therefore, have

669   lower nutritional content.

670

671   Among the array of fatty acids synthesized in algal communities, essential fatty acids (EFAs) are

672   most likely to be taxonomically associated with, and influenced by, changing community

673   composition. EFAs are a subgroup of polyunsaturated fatty acids (PUFAs) that are prone to

674   accumulating in organisms (see Kelly & Scheibling, 2012). Among the eight common EFAs

675   (Taipale et al. 2013), 18:3ω3, 18:2ω6, and 20:5ω3 had the highest coefficients of variation

676   between sites. Because these three EFAs demonstrated the greatest variation between sites, our

677   analyses focused on how their relative abundances related to PPCP concentrations and IDW

678   populations. The fatty acids 18:3ω3 and 18:2ω6 have been previously associated with

679   filamentous algae, such as Baikalian *Ulothrix* (Osipova et al. 2009), whereas 20:5ω3 have

680   previously been associated with Baikalian diatoms (Shishlyannikov et al. 2018). Comparing the

681   ratio of filamentous green algae to diatoms could therefore function as proxy for each algal

682   taxon's relative abundance and potentially offer insights into feeding patterns for the grazers.

683

684   *Relating sewage indicators with macroinvertebrate feeding guilds*

685   In assessing benthic consumer communities' responses to changing periphyton, our data suggest

686   macroinvertebrate guilds reshape with increasing sewage pollution. Our results support the

687   general conclusion of Timoshkin et al. (2016) that Baikalian mollusk abundance tends to

688   decrease with increasing sewage pollution. Decreased mollusk abundance may have several

689   causes, including low tolerance for increased concentrations of PPCPs or other components of

690   sewage (e.g., Hollingsworth et al. 2002, Timoshkin et al. 2016), inability to consume filamentous

691   algae (Mazzella and Russo 1989), or filamentous algae not offering the proper nutrition (Lowe

692   and Hunter 1988). In contrast to mollusks, amphipods were generally prevalent at all littoral

693   sites, regardless of sewage indicator concentrations. *Brandtia* spp. was the only amphipod genus

694   less abundant with sewage indicator signals. This genus tends to be associated with endemic

695   sponges (Taakhteev & Didorenko, 2015), which may also be decreasing in abundance near areas

696   of lakeside development (Timoshkin et al., 2016). *Eulimnogammarus* spp., one of the most

697   speciose Baikal genera (Takhteev and Didorenko 2015), was prevalent at all sites, and δ^{15}N

698   values in its tissue increased slightly but significantly with increasing IDW population. Unlike

699   periphyton, amphipods' increasing δ^{15}N values may relate to amphipods having longer cellular

700   turnover rates (e.g., weeks; McIntyre and Flecker 2006) relative to periphyton. Consequently,

701   amphipods' enhanced δ^{15}N values suggest that sewage-derived nutrients are being incorporated

702   into the food web. While we did not test amphipod tissues for other sewage indicators such as

703   PPCPs and microplastics, the potential for PPCPs to bioaccumulate and biomagnify in food webs

704   has been recently demonstrated, with ecological ramifications remaining uncertain (Lagesson et

705   al., 2016; Richmond et al., 2018). These combined results suggest that mollusk abundance and

706   amphipod δ^{15}N values may be longer-term indicators of sewage pollution in Baikal.

707

708   In contrast to variation in δ^{15}N values, amphipod fatty acid profiles did not differ markedly

709   between sites (Figure 7). Amphipods from all collected sites expressed consistent 20:5ω3

710   signatures relative to 18:3ω3 and 18:2ω6. Consumers usually accumulate fatty acids from their

711   food source. Yoshii's (1999) study as well as our own stable isotope data suggest that Baikal's

712   benthic, littoral amphipods are likely a combination of grazers and omnivores. Because fatty acid

713   profiles in amphipods largely reflected fatty acid signatures in periphyton, our data suggest that

714   amphipods likely continue grazing on periphyton, despite the food resource changing in

715   community composition and nutritional content. As a consequence, amphipods may be

716   compensating for the shifting nutritional quality of periphyton through at least two potential

717 mechanisms. First, amphipods may selectively consume diatoms as opposed to filamentous

718 algae, meaning diatom relative abundance could decrease both from increased grazing and lesser

719 efficiency at taking up nutrients relative to filamentous taxa. Second, amphipods themselves

720 (e.g., Desvilettes et al. 1997; Castell et al. 2004) or heterotrophic symbionts (Klein Breteler et al.

721 1999; Veloza et al. 2006; Hiltunen et al. 2017) may upgrade fatty acids by investing energy to

722 convert C18 fatty acids to C20 fatty acids. Regardless of the exact mechanism, our data suggest

723 that food web interactions would change with increasing sewage pollution and may imply a net

724 energetic cost through amphipods' differential grazing patterns.

725

726 *Conclusions*

727 Over the past decade, Lake Baikal has shown signs of nearshore eutrophication, despite the

728 pelagic zone remaining ultra-oligotrophic. While Baikal receives nutrients from multiple sources,

729 sewage-specific indicators used in this study implicate wastewater pollution as one of the

730 sources. Our results corroborate work by Timoshkin et al. (2016, 2018), demonstrating how

731 patchy hot spots of lakeside development at Baikal can create gradients in sewage concentrations

732 and ecological responses. Unlike previous studies, our approach pairs community abundance

733 data (i.e., periphyton and macroinvertebrate counts) and nuanced dietary tracers (i.e., fatty acids)

734 to assess benthic community and food web consequences of sewage pollution. While sewage

735 pollution may lead to changing resources for macroinvertebrate grazers, Baikal's amphipods

736 appear to be compensating either (1) by selectively grazing on diatoms or (2) by consuming less

737 desirable food and upgrading fatty acids. In both cases, our results suggest shifting community

738 interactions and may imply a net energetic cost for amphipods, as they expend energy either by

739 foraging selectively for diatoms or by catabolizing certain essential fatty acids.

740

Future trajectories: a call for increased nearshore monitoring

Our results underscore the importance of nearshore monitoring in detecting sewage pollution in large lakes. Lake Baikal is considered ultra-oligotrophic based on pelagic sampling (Yoshida et al. 2003; O'Donnell et al. 2017), but nearshore hot spots of eutrophication are developing throughout the lake (Timoshkin et al. 2016, 2018). While pelagic samples are representative of the lake's overall status, nearshore sampling aids managers in identifying pollution loading before the entire system is affected (Jacoby et al. 1991; Lambert et al. 2008; Hampton et al. 2011). Beyond Baikal, several large, deep, oligotrophic lakes have likewise experienced localized sewage pollution with nearshore biological responses, despite pelagic measurements suggesting oligotrophic status (e.g., Jacoby et al. 1991, Rosenberger et al. 2008; Hampton et al., 2011). Once eutrophication of the open water has occurred, mitigation can involve complex socio-economic factors (Carpenter et al. 1999), require system-specific information (Jeppesen et al. 2005), and necessitate long-term strategies (Tong et al. 2020). Because nutrients may enter systems from numerous sources, incorporating sewage specific indicators, such as PPCPs, may be necessary. PPCP sampling has the potential to not only identify sewage-associated nutrient pollution but also assess heterogeneities in sewage loading along a shoreline. When PPCP data are paired with co-located benthic community composition and food web data, managers can take system-specific actions to mitigate ecological consequences before sewage concentrations are detected throughout the lake. Across larger spatial and temporal scales, these paired PPCP-biological samples have potential to offer a synoptic view of the impacts of sewage pollution, enabling regional and local monitoring to coordinate mitigation strategies

762

763

Works Cited

765 Anderson, M. J. 2001. A new method for non-parametric multivariate analysis of variance. Austral

766   Ecology **26**: 32–46. doi:10.1111/j.1442-9993.2001.01070.pp.x

767 Andersson, E., and A.-K. Brunberg. 2006. Inorganic nutrient acquisition in a shallow clearwater lake –

768   dominance of benthic microbiota. Aquatic Sciences **68**: 172–180. doi:10.1007/s00027-006-0805-

769   x

770 Anisimov, O., and S. Reneva. 2006. Permafrost and Changing Climate: The Russian Perspective. Ambio

771   **35**: 169–175.

772 Barnes, D. K. A., F. Galgani, R. C. Thompson, and M. Barlaz. 2009. Accumulation and fragmentation of

773   plastic debris in global environments. Philos Trans R Soc Lond B Biol Sci **364**: 1985–1998.

774   doi:10.1098/rstb.2008.0205

775 Bendz, D., N. A. Paxéus, T. R. Ginn, and F. J. Loge. 2005. Occurrence and fate of pharmaceutically

776   active compounds in the environment, a case study: Höje River in Sweden. Journal of Hazardous

777   Materials **122**: 195–204. doi:10.1016/j.jhazmat.2005.03.012

778 Brandon, J. A., A. Freibott, and L. M. Sala. 2020. Patterns of suspended and salp-ingested microplastic

779   debris in the North Pacific investigated with epifluorescence microscopy. Limnology and

780   Oceanography Letters **5**: 46–53. doi:10.1002/lol2.10127

781 Brandon, J., M. Goldstein, and M. D. Ohman. 2016. Long-term aging and degradation of microplastic

782   particles: Comparing in situ oceanic and experimental weathering patterns. Marine Pollution

783   Bulletin **110**: 299–308. doi:10.1016/j.marpolbul.2016.06.048

784 Brodin, T., J. Fick, M. Jonsson, and J. Klaminder. 2013. Dilute concentrations of a psychiatric drug alter

785   behavior of fish from natural populations. Science **339**: 814–815. doi:10.1126/science.1226850

786 Camilleri, A. C., and T. Ozersky. 2019. Large variation in periphyton δ^{13}C and δ^{15}N values in the upper

787 Great Lakes: Correlates and implications. Journal of Great Lakes Research **45**: 986–990.

788 doi:10.1016/j.jglr.2019.06.003

789 Carpenter, S. R., D. Ludwig, and W. A. Brock. 1999. Management of eutrophication for lakes subject to

790 potentially irreversible change. Ecological Applications **9**: 751–771. doi:10.2307/2641327

791 Castell, J. D., E. J. Kennedy, S. M. C. Robinson, G. J. Parsons, T. J. Blair, and E. Gonzalez-Duran. 2004.

792 Effect of dietary lipids on fatty acid composition and metabolism in juvenile green sea urchins

793 (Strongylocentrotus droebachiensis). Aquaculture **242**: 417–435.

794 doi:10.1016/j.aquaculture.2003.11.003

795 Chang, H.-Y., S.-H. Wu, K.-T. Shao, and others. 2012. Longitudinal variation in food sources and their

796 use by aquatic fauna along a subtropical river in Taiwan. Freshwater Biology **57**: 1839–1853.

797 doi:10.1111/j.1365-2427.2012.02843.x

798 Clarke, K. R. 1993. Non-parametric multivariate analyses of changes in community structure. Australian

799 Journal of Ecology **18**: 117–143. doi:https://doi.org/10.1111/j.1442-9993.1993.tb00438.x

800 Cole, M. L., I. Valiela, K. D. Kroeger, and others. 2004. Assessment of a δ^{15}N isotopic method to indicate

801 anthropogenic eutrophication in aquatic ecosystems. J. Environ. Qual. **33**: 124–132.

802 doi:10.2134/jeq2004.1240

803 Costanzo, S. D., M. J. O'Donohue, W. C. Dennison, N. R. Loneragan, and M. Thomas. 2001. A new

804 approach for detecting and mapping sewage impacts. Marine Pollution Bulletin **42**: 149–156.

805 doi:10.1016/S0025-326X(00)00125-9

806 Craine, J. M., A. J. Elmore, L. Wang, and others. 2018. Isotopic evidence for oligotrophication of

807 terrestrial ecosystems. Nature Ecology & Evolution **2**: 1735–1744. doi:10.1038/s41559-018-

808 0694-0

809 Czekalski, N., R. Sigdel, J. Birtel, B. Matthews, and H. Bürgmann. 2015. Does human activity impact the

810 natural antibiotic resistance background? Abundance of antibiotic resistance genes in 21 Swiss

811 lakes. Environment International **81**: 45–55. doi:10.1016/j.envint.2015.04.005

812   D'Alessio, M., S. Onanong, D. D. Snow, and C. Ray. 2018. Occurrence and removal of pharmaceutical

813   compounds and steroids at four wastewater treatment plants in Hawai'i and their environmental

814   fate. Science of The Total Environment **631–632**: 1360–1370.

815   doi:10.1016/j.scitotenv.2018.03.100

816   Dalsgaard, J., M. St. John, G. Kattner, D. Müller-Navarra, and W. Hagen. 2003. Fatty acid trophic

817   markers in the pelagic marine environment, p. 225–340. *In* Advances in Marine Biology.

818   Elsevier.

819   Desvilettes, Ch., G. Bourdier, and J. Ch. Breton. 1997. On the occurrence of a possible bioconversion of

820   linolenic acid into docosahexaenoic acid by the copepod *Eucyclops serrulatus* fed on microalgae.

821   J Plankton Res **19**: 273–278. doi:10.1093/plankt/19.2.273

822   Dzieweczynski, T. L., B. A. Campbell, and J. L. Kane. 2016. Dose-dependent fluoxetine effects on

823   boldness in male Siamese fighting fish. Journal of Experimental Biology **219**: 797–804.

824   doi:10.1242/jeb.132761

825   Eerkes-Medrano, D., R. C. Thompson, and D. C. Aldridge. 2015. Microplastics in freshwater systems: A

826   review of the emerging threats, identification of knowledge gaps and prioritisation of research

827   needs. Water Research **75**: 63–82. doi:10.1016/j.watres.2015.02.012

828   Eriksen, M., S. Mason, S. Wilson, C. Box, A. Zellers, W. Edwards, H. Farley, and S. Amato. 2013.

829   Microplastic pollution in the surface waters of the Laurentian Great Lakes. Marine Pollution

830   Bulletin **77**: 177–182. doi:10.1016/j.marpolbul.2013.10.007

831   Feijão, E., R. Cruz de Carvalho, I. A. Duarte, and others. 2020. Fluoxetine arrests growth of the model

832   diatom *Phaeodactylum tricornutum* by increasing oxidative stress and altering energetic and lipid

833   metabolism. Front Microbiol **11**. doi:10.3389/fmicb.2020.01803

834   Fellows, I., and using the Jm. library by J. P. Stotz. 2019. OpenStreetMap: Access to Open Street Map

835   Raster Images,.

836   Firke, S. 2020. janitor: Simple Tools for Examining and Cleaning Dirty Data.

837   Fischer, E. K., L. Paglialonga, E. Czech, and M. Tamminga. 2016. Microplastic pollution in lakes and

838   lake shoreline sediments – A case study on Lake Bolsena and Lake Chiusi (central Italy).

839   Environmental Pollution **213**: 648–657. doi:10.1016/j.envpol.2016.03.012

840   Focazio, M. J., D. W. Kolpin, K. K. Barnes, E. T. Furlong, M. T. Meyer, S. D. Zaugg, L. B. Barber, and

841   M. E. Thurman. 2008. A national reconnaissance for pharmaceuticals and other organic

842   wastewater contaminants in the United States - II) Untreated drinking water sources. Science of

843   the Total Environment **402**: 201–216. doi:10.1016/j.scitotenv.2008.02.021

844   Free, C. M., O. P. Jensen, S. A. Mason, M. Eriksen, N. J. Williamson, and B. Boldgiv. 2014. High-levels

845   of microplastic pollution in a large, remote, mountain lake. Marine Pollution Bulletin **85**: 156–

846   163. doi:10.1016/j.marpolbul.2014.06.001

847   Galloway, A. W. E., and M. Winder. 2015. Partitioning the relative importance of phylogeny and

848   environmental conditions on phytoplankton fatty acids. PLOS ONE **10**: e0130053.

849   doi:10.1371/journal.pone.0130053

850   Galloway, J. N., F. J. Dentener, D. G. Capone, and others. 2004. Nitrogen cycles: Past, present, and

851   future. biogeochemistry **70**: 153–226. doi:10.1007/s10533-004-0370-0

852   Garnier, S. 2018. viridis: Default Color Maps from "matplotlib."

853   Gartner, A., P. Lavery, and A. J. Smit. 2002. Use of δ^{15}N signatures of different functional forms of

854   macroalgae and filter-feeders to reveal temporal and spatial patterns in sewage dispersal. Mar.

855   Ecol.-Prog. Ser. **235**: 63–73. doi:10.3354/meps235063

856   Green, D. S. 2016. Effects of microplastics on European flat oysters, *Ostrea edulis* and their associated

857   benthic communities. Environmental Pollution **216**: 95–103. doi:10.1016/j.envpol.2016.05.043

858   Guzzo, M. M., G. D. Haffner, S. Sorge, S. A. Rush, and A. T. Fisk. 2011. Spatial and temporal

859   variabilities of δ^{13}C and δ^{15}N within lower trophic levels of a large lake: implications for

860   estimating trophic relationships of consumers. Hydrobiologia **675**: 41–53. doi:10.1007/s10750-

861   011-0794-1

862 Hadwen, W. L., and S. E. Bunn. 2005. Food web responses to low-level nutrient and δ^{15}N-tracer additions

863   in the littoral zone of an oligotrophic dune lake. Limnology and Oceanography **50**: 1096.

864 Hampton, S. E., S. C. Fradkin, P. R. Leavitt, and E. E. Rosenberger. 2011. Disproportionate importance

865   of nearshore habitat for the food web of a deep oligotrophic lake. Marine and Freshwater

866   Research **62**: 350. doi:10.1071/MF10229

867 Hampton, S. E., S. McGowan, T. Ozersky, and others. 2018. Recent ecological change in ancient lakes.

868   Limnology and Oceanography **63**: 2277–2304. doi:10.1002/lno.10938

869 Hanvey, J. S., P. J. Lewis, J. L. Lavers, N. D. Crosbie, K. Pozo, and B. O. Clarke. 2017. A review of

870   analytical techniques for quantifying microplastics in sediments. Anal. Methods **9**: 1369–1383.

871   doi:10.1039/C6AY02707E

872 Hendrickson, E., E. C. Minor, and K. Schreiner. 2018. Microplastic abundance and composition in

873   western lake superior as determined via microscopy, Pyr-GC/MS, and FTIR. Environ. Sci.

874   Technol. **52**: 1787–1796. doi:10.1021/acs.est.7b05829

875 Hester, J., and H. Wickham. 2019. fs: Cross-Platform File System Operations Based on "libuv."

876 Hiltunen, M., M. Honkanen, S. Taipale, U. Strandberg, and P. Kankaala. 2017. Trophic upgrading via the

877   microbial food web may link terrestrial dissolved organic matter to Daphnia. J Plankton Res **39**:

878   861–869. doi:10.1093/plankt/fbx050

879 Hollingsworth, R. G., J. W. Armstrong, and E. Campbell. 2002. Caffeine as a repellent for slugs and

880   snails. Nature **417**: 915–916. doi:10.1038/417915a

881 Interfax-Tourism. 2018. Байкал с января по август 2018 года посетили 1,2 миллиона туристов (1.2

882   million tourists visited Baikal from January through August 2018). Interfax-Tourism, October 25

883 Iverson, S. J., C. Field, W. D. Bowen, and W. Blanchard. 2004. Quantitative Fatty Acid Signature

884   Analysis: A New Method of Estimating Predator Diets. Ecological Monographs **74**: 211–235.

885   doi:10.1890/02-4105

886 Izhboldina, L. A. 2007. Guide and Key to Benthic and Periphyton Algae of Lake Baikal (meio- and

887   macrophytes) with Brief Notes on Their Ecology, Nauka-Centre.

888 Jacoby, J. M., D. D. Bouchard, and C. R. Patmont. 1991. Response of periphyton to nutrient enrichment

889   in Lake Chelan, WA. Lake and Reservoir Management **7**: 33–43.

890   doi:10.1080/07438149109354252

891 Jeppesen, E., M. Søndergaard, J. P. Jensen, and others. 2005. Lake responses to reduced nutrient loading

892   – an analysis of contemporary long-term data from 35 case studies. Freshwater Biology **50**:

893   1747–1771. doi:10.1111/j.1365-2427.2005.01415.x

894 Johnson, R. A., and D. V. Wichern. 2007. Applied Multivariate Statistical Analysis, 6th ed. Prentice Hall.

895 Karnaukhov, D., S. Biritskaya, E. Dolinskaya, M. Teplykh, N. Silenko, Y. Ermolaeva, and E. Silow.

896   2020. Pollution by macro- and microplastic of large lacustrine ecosystems in eastern Asia.

897   Pollution Research **2**: 353–355.

898 Karnjanapiboonwong, A., A. N. Morse, J. D. Maul, and T. A. Anderson. 2010. Sorption of estrogens,

899   triclosan, and caffeine in a sandy loam and a silt loam soil. Journal of Soils and Sediments **10**:

900   1300–1307. doi:10.1007/s11368-010-0223-5

901 Kassambara, A. 2019. ggpubr: "ggplot2" Based Publication Ready Plots,.

902 Kassambara, A., and F. Mundt. 2019. factoextra: Extract and Visualize the Results of Multivariate Data

903   Analyses,.

904 Kaufman, L., and P. J. Rousseeuw. 2005. Finding Groups in Data: An Introduction to Cluster Analysis,

905   1st Edition. Wiley-Interscience.

906 Kelly, J. R., and R. E. Scheibling. 2012. Fatty acids as dietary tracers in benthic food webs. Marine

907   Ecology Progress Series **446**: 1–22. doi:10.3354/meps09559

908 Klein Breteler, W. C. M., N. Schogt, M. Baas, S. Schouten, and G. W. Kraay. 1999. Trophic upgrading of

909   food quality by protozoans enhancing copepod growth: role of essential lipids. Marine Biology

910   **135**: 191–198. doi:10.1007/s002270050616

911 Klein, S., E. Worch, and T. P. Knepper. 2015. Occurrence and spatial distribution of microplastics in river

912   shore sediments of the Rhine-Main area in Germany. Environ. Sci. Technol. **49**: 6070–6076.

913   doi:10.1021/acs.est.5b00492

914   Kolpin, D. W., E. T. Furlong, M. T. Meyer, E. M. Thurman, S. D. Zaugg, L. B. Barber, and H. T. Buxton.

915   2002. Pharmaceuticals, hormones, and other organic wastewater contaminants in u.s. streams,

916   1999−2000: A national reconnaissance. Environmental Science & Technology **36**: 1202–1211.

917   doi:10.1021/es011055j

918   Kozhov, M. M. 1963. Lake Baikal and its Life, Springer Science & Business Media.

919   Kozhova, O. M., and L. R. Izmest'eva. 1998. Lake Baikal: Evolution and Biodiversity, Backhuys

920   Publishers.

921   Kravtsova, L. S., L. A. Izhboldina, I. V. Khanaev, and others. 2014. Nearshore benthic blooms of

922   filamentous green algae in Lake Baikal. Journal of Great Lakes Research **40**: 441–448.

923   doi:10.1016/j.jglr.2014.02.019

924   Lagesson, A., J. Fahlman, T. Brodin, J. Fick, M. Jonsson, P. Byström, and J. Klaminder. 2016.

925   Bioaccumulation of five pharmaceuticals at multiple trophic levels in an aquatic food web -

926   Insights from a field experiment. Science of The Total Environment **568**: 208–215.

927   doi:10.1016/j.scitotenv.2016.05.206

928   Lambert, D., A. Cattaneo, and R. Carignan. 2008. Periphyton as an early indicator of perturbation in

929   recreational lakes. Can. J. Fish. Aquat. Sci. **65**: 258–265. doi:10.1139/f07-168

930   Legendre, P., and L. Legendre. 2012. Numerical Ecology, 3rd ed. Elsevier.

931   Li, J., C. Green, A. Reynolds, H. Shi, and J. M. Rotchell. 2018. Microplastics in mussels sampled from

932   coastal waters and supermarkets in the United Kingdom. Environmental Pollution **241**: 35–44.

933   doi:10.1016/j.envpol.2018.05.038

934   Lorenzen, C. J. 1967. Determination of chlorophyll and pheo-pigments: Spectrophotometric equations1.

935   Limnology and Oceanography **12**: 343–346. doi:https://doi.org/10.4319/lo.1967.12.2.0343

936   Lowe, R. L., and R. D. Hunter. 1988. Effect of grazing by Physa integra on periphyton community

937   structure. Journal of the North American Benthological Society **7**: 29–36. doi:10.2307/1467828

938   Maechler, M., P. Rousseeuw, A. Struyf, M. Hubert, and K. Hornik. 2019. cluster: Cluster Analysis Basics

939   and Extensions,.

940   Mazzella, L., and G. F. Russo. 1989. Grazing effect of two Gibbula species (Mollusca,

941   Archaeogastropoda) on the epiphytic community of Posidonia oceanica leaves.

942   McIntyre, P. B., and A. S. Flecker. 2006. Rapid turnover of tissue nitrogen of primary consumers in

943   tropical freshwaters. Oecologia **148**: 12–21. doi:10.1007/s00442-005-0354-3

944   Meyer, M. F., T. Ozersky, K. H. Woo, and others. 2020. A unified dataset of co-located sewage pollution,

945   periphyton, and benthic macroinvertebrate community and food web structure from Lake Baikal

946   (Siberia).doi:10.6073/PASTA/76F43144015EC795679BAC508EFA044B

947   Meyer, M. F., S. M. Powers, and S. E. Hampton. 2019. An evidence synthesis of pharmaceuticals and

948   personal care products (PPCPs) in the environment: Imbalances among compounds, sewage

949   treatment techniques, and ecosystem types. Environ. Sci. Technol. **53**: 12961–12973.

950   doi:10.1021/acs.est.9b02966

951   Meyer, M., T. Ozersky, K. Woo, A. W. E. Galloway, M. R. Brousil, and S. Hampton. 2015. Baikal Food

952   Webs. doi:10.17605/OSF.IO/9TA8Z

953   Monteith, D. T., J. L. Stoddard, C. D. Evans, and others. 2007. Dissolved organic carbon trends resulting

954   from changes in atmospheric deposition chemistry. Nature **450**: 537–540.

955   doi:10.1038/nature06316

956   Moore, J. W., D. E. Schindler, M. D. Scheuerell, D. Smith, and J. Frodge. 2003. Lake eutrophication at

957   the urban fringe, Seattle region, USA. AMBIO: A Journal of the Human Environment **32**: 13–18.

958   Moore, M. V., S. E. Hampton, L. R. Izmest'eva, E. A. Silow, E. V. Peshkova, and B. K. Pavlov. 2009.

959   Climate Change and the World's "Sacred Sea"-Lake Baikal, Siberia. Bioscience **59**: 405–417.

960   doi:10.1525/bio.2009.59.5.8

961   Moran, P. W., S. E. Cox, S. S. Embrey, R. L. Huffman, T. D. Olsen, and S. C. Fradkin. 2012. Sources and

962   Sinks of Nitrogen and Phosphorus in a Deep, Oligotrophic Lake, Lake Crescent, Olympic

963   National Park, Washington. US Geological Survey.

964   O'Donnell, D. R., P. Wilburn, E. A. Silow, L. Y. Yampolsky, and E. Litchman. 2017. Nitrogen and

965   phosphorus colimitation of phytoplankton in Lake Baikal: Insights from a spatial survey and

966   nutrient enrichment experiments. Limnology and Oceanography **62**: 1383–1392.

967   doi:10.1002/lno.10505

968   Oksanen, J., F. G. Blanchet, M. Friendly, and others. 2019. vegan: Community Ecology Package,.

969   Osipova, S., L. Dudareva, N. Bondarenko, A. Nasarova, N. Sokolova, L. Obolkina, O. Glyzina, and O.

970   Timoshkin. 2009. Temporal variation in fatty acid composition of *Ulothrix zonata* (Chlorophyta)

971   from ice and benthic communities of Lake Baikal. Phycologia **48**: 130–135.

972   Ozersky, T., E. A. Volkova, N. A. Bondarenko, O. A. Timoshkin, V. V. Malnik, V. M. Domysheva, and

973   S. E. Hampton. 2018. Nutrient limitation of benthic algae in Lake Baikal, Russia. Freshwater

974   Science **37**: 472–482. doi:10.1086/699408

975   Parsons, T. R., and J. D. H. Strickland. 1963. Discussion of spectrophotometric determination of marine-

976   plant pigments, with revised equations for ascertaining chlorophylls and carotenoids. Journal of

977   Marine Research.

978   Pebesma, E. 2018. Simple Features for R: Standardized Support for Spatial Vector Data. The R Journal

979   **10**: 439–446. doi:10.32614/RJ-2018-009

980   Piñón-Gimate, A., M. F. Soto-Jiménez, M. J. Ochoa-Izaguirre, E. García-Pagés, and F. Páez-Osuna. 2009.

981   Macroalgae blooms and δ^{15}N in subtropical coastal lagoons from the Southeastern Gulf of

982   California: Discrimination among agricultural, shrimp farm and sewage effluents. Marine

983   Pollution Bulletin **58**: 1144–1151. doi:10.1016/j.marpolbul.2009.04.004

984   Powers, S. M., T. W. Bruulsema, T. P. Burt, and others. 2016. Long-term accumulation and transport of

985   anthropogenic phosphorus in three river basins. Nature Geoscience **9**: 353–356.

986   doi:10.1038/ngeo2693

987   R Core Team. 2019. R: A Language and Environment for Statistical Computing,.

988   del Rey, Z. R., E. F. Granek, and B. A. Buckley. 2011. Expression of HSP70 in *Mytilus californianus*

989   following exposure to caffeine. Ecotoxicology **20**: 855–861. doi:10.1007/s10646-011-0649-6

990   Richmond, E. K., E. J. Rosi, A. J. Reisinger, B. R. Hanrahan, R. M. Thompson, and M. R. Grace. 2019.

991   Influences of the antidepressant fluoxetine on stream ecosystem function and aquatic insect

992   emergence at environmentally realistic concentrations. Journal of Freshwater Ecology **34**: 513–

993   531. doi:10.1080/02705060.2019.1629546

994 Richmond, E. K., E. J. Rosi, D. M. Walters, J. Fick, S. K. Hamilton, T. Brodin, A. Sundelin, and M. R.

995   Grace. 2018. A diverse suite of pharmaceuticals contaminates stream and riparian food webs.

996   Nature Communications **9**: 4491. doi:10.1038/s41467-018-06822-w

997 Risk, M. J., B. E. Lapointe, O. A. Sherwood, and B. J. Bedford. 2009. The use of δ^{15}N in assessing

998   sewage stress on coral reefs. Marine Pollution Bulletin **58**: 793–802.

999   doi:10.1016/j.marpolbul.2009.02.008

1000 Robson, S. V., E. J. Rosi, E. K. Richmond, and M. R. Grace. 2020. Environmental concentrations of

1001   pharmaceuticals alter metabolism, denitrification, and diatom assemblages in artificial streams.

1002   Freshwater Science **39**: 256–267. doi:10.1086/708893

1003 Romera-Castillo, C., M. Pinto, T. M. Langer, X. A. Álvarez-Salgado, and G. J. Herndl. 2018. Dissolved

1004   organic carbon leaching from plastics stimulates microbial activity in the ocean. Nat Commun **9**:

1005   1–7. doi:10.1038/s41467-018-03798-5

1006 Rosenberger, E. E., S. E. Hampton, S. C. Fradkin, and B. P. Kennedy. 2008. Effects of shoreline

1007   development on the nearshore environment in large deep oligotrophic lakes. Freshwater Biology

1008   **53**: 1673–1691. doi:10.1111/j.1365-2427.2008.01990.x

1009 Rosi-Marshall, E. J., D. W. Kincaid, H. A. Bechtold, T. V. Royer, M. Rojas, and J. J. Kelly. 2013.

1010   Pharmaceuticals suppress algal growth and microbial respiration and alter bacterial communities

1011   in stream biofilms. Ecological Applications **23**: 583–593. doi:10.1890/12-0491.1

1012 Rosi-Marshall, E. J., and T. V. Royer. 2012. Pharmaceutical compounds and ecosystem function: An

1013   emerging research challenge for aquatic ecologists. Ecosystems **15**: 867–880.

1014   doi:10.1007/s10021-012-9553-z

1015 Sargent, J. R., and S. Falk-Petersen. 1988. The lipid biochemistry of calanoid copepods. Hydrobiologia

1016   **167–168**: 101–114. doi:10.1007/BF00026297

1017   Savage, C., and R. Elmgren. 2004. Macroalgal (*Fucus vesiculosus*) δ^{15}N values trace decrease in sewage

1018   influence. Ecological Applications **14**: 517–526. doi:10.1890/02-5396

1019   Schram, J. B., J. N. Kobelt, M. N. Dethier, and A. W. E. Galloway. 2018. Trophic transfer of macroalgal

1020   fatty acids in two urchin species: Digestion, egestion, and tissue building. Front. Ecol. Evol. **6**.

1021   doi:10.3389/fevo.2018.00083

1022   Shishlyannikov, S. M., A. A. Nikonova, Y. S. Bukin, and A. G. Gorshkov. 2018. Fatty acid trophic

1023   markers in Lake Baikal phytoplankton: A comparison of endemic and cosmopolitan diatom-

1024   dominated phytoplankton assemblages. Ecological Indicators **85**: 878–886.

1025   doi:10.1016/j.ecolind.2017.11.052

1026   Sitnikova, T. Ya. 2012. Определитель брюхоногих моллюсков бухты Большие Коты (юго-западное

1027   побережье озера Байкал) [Key of the Gastropod Molluscs in the Bay of Bolshie Koty (South-

1028   West shoreline of Lake Baikal)], Irkutsk State University.

1029   Slowikowski, K. 2019. ggrepel: Automatically Position Non-Overlapping Text Labels with "ggplot2,."

1030   Smith, V. H., G. D. Tilman, and J. C. Nekola. 1999. Eutrophication: Impacts of excess nutrient inputs on

1031   freshwater, marine, and terrestrial ecosystems. Environmental Pollution **100**: 179–196.

1032   doi:10.1016/S0269-7491(99)00091-3

1033   Sneath, P. H. A., and R. R. Sokal. 1973. Numerical Taxonomy: The Principles and Practice of Numerical

1034   Classification, W. H. Freeman.

1035   Steinmetz, Z., C. Wollmann, M. Schaefer, and others. 2016. Plastic mulching in agriculture: Trading

1036   short-term agronomic benefits for long-term soil degradation? Science of The Total Environment

1037   **550**: 690–705. doi:10.1016/j.scitotenv.2016.01.153

1038   Stoddard, J. L., J. Van Sickle, A. T. Herlihy, J. Brahney, S. Paulsen, D. V. Peck, R. Mitchell, and A. I.

1039   Pollard. 2016. Continental-scale increase in lake and stream phosphorus: Are oligotrophic

1040   systems disappearing in the united states? Environ. Sci. Technol. **50**: 3409–3415.

1041   doi:10.1021/acs.est.5b05950

1042   Sumner, M. D. 2019. spdplyr: Data Manipulation Verbs for the Spatial Classes,.

1043   Suzuki, R., Y. Terada, and H. Shimodaira. 2019. pvclust: Hierarchical Clustering with P-Values via

1044   Multiscale Bootstrap Resampling,.

1045   Swamikannu, X., and K. D. Hoagland. 1989. Effects of snail grazing on the diversity and structure of a

1046   periphyton community in a eutrophic pond. Can. J. Fish. Aquat. Sci. **46**: 1698–1704.

1047   doi:10.1139/f89-215

1048   Swann, G. E. A., V. N. Panizzo, S. Piccolroaz, and others. 2020. Changing nutrient cycling in Lake

1049   Baikal, the world's oldest lake. PNAS **117**: 27211–27217. doi:10.1073/pnas.2013181117

1050   Taipale, S., U. Strandberg, E. Peltomaa, A. W. E. Galloway, A. Ojala, and M. T. Brett. 2013. Fatty acid

1051   composition as biomarkers of freshwater microalgae: Analysis of 37 strains of microalgae in 22

1052   genera and in seven classes. Aquatic Microbial Ecology **71**: 165–178. doi:10.3354/ame01671

1053   Takhteev, V. V., and D. I. Didorenko. 2015. Fauna and ecology of amphipods of Lake Baikal: A Training

1054   manual, V.B. Sochava Institute of Geography SB RAS.

1055   Timoshkin, O. A., M. V. Moore, N. N. Kulikova, and others. 2018. Groundwater contamination by

1056   sewage causes benthic algal outbreaks in the littoral zone of Lake Baikal (East Siberia). Journal

1057   of Great Lakes Research. doi:10.1016/j.jglr.2018.01.008

1058   Timoshkin, O. A., D. P. Samsonov, M. Yamamuro, and others. 2016. Rapid ecological change in the

1059   coastal zone of Lake Baikal (East Siberia): Is the site of the world's greatest freshwater

1060   biodiversity in danger? Journal of Great Lakes Research **42**: 487–497.

1061   doi:10.1016/j.jglr.2016.02.011

1062   Tong, Y., M. Wang, J. Peñuelas, and others. 2020. Improvement in municipal wastewater treatment alters

1063   lake nitrogen to phosphorus ratios in populated regions. Proc Natl Acad Sci USA **117**: 11566–

1064   11572. doi:10.1073/pnas.1920759117

1065   Tornqvist, R., J. Jarsjo, J. Pietron, A. Bring, P. Rogberg, S. M. Asokan, and G. Destouni. 2014. Evolution

1066   of the hydro-climate system in the Lake Baikal basin. Journal of Hydrology **519**: 1953–1962.

1067   doi:10.1016/j.jhydrol.2014.09.074

1068 Turetsky, M. R., R. K. Wieder, C. J. Williams, and D. H. Vitt. 2000. Organic matter accumulation, peat

1069   chemistry, and permafrost melting in peatlands of boreal Alberta. Écoscience **7**: 115–122.

1070   doi:10.1080/11956860.2000.11682608

1071 Veloza, A. J., F.-L. E. Chu, and K. W. Tang. 2006. Trophic modification of essential fatty acids by

1072   heterotrophic protists and its effects on the fatty acid composition of the copepod *Acartia tonsa*.

1073   Marine Biology **148**: 779–788. doi:10.1007/s00227-005-0123-1

1074 Volkova, E. A., N. A. Bondarenko, and O. A. Timoshkin. 2018. Morphotaxonomy, distribution and

1075   abundance of *Spirogyra* (Zygnematophyceae, Charophyta) in Lake Baikal, East Siberia.

1076   Phycologia **57**: 298–308. doi:10.2216/17-69.1

1077 de Vries, J. 1972. Soil filtration of wastewater effluent and the mechanism of pore clogging. Journal

1078   (Water Pollution Control Federation) **44**: 565–573.

1079 Wang, W., and J. Wang. 2018. Investigation of microplastics in aquatic environments: An overview of

1080   the methods used, from field sampling to laboratory analysis. TrAC Trends in Analytical

1081   Chemistry **108**: 195–202. doi:10.1016/j.trac.2018.08.026

1082 Wayland, M., and K. A. Hobson. 2001. Stable carbon, nitrogen, and sulfur isotope ratios in riparian food

1083   webs on rivers receiving sewage and pulp-mill effluents. Can. J. Zool. **79**: 5–15. doi:10.1139/z00-

1084   169

1085 Wickham, H., M. Averick, J. Bryan, and others. 2019. Welcome to the tidyverse. Journal of Open Source

1086   Software **4**: 1686. doi:10.21105/joss.01686

1087 Wilke, C. O. 2019. cowplot: Streamlined Plot Theme and Plot Annotations for "ggplot2,."

1088 Wilke, C. O. 2020. ggtext: Improved Text Rendering Support for "ggplot2,."

1089 Yang, Y., W. Song, H. Lin, W. Wang, L. Du, and W. Xing. 2018. Antibiotics and antibiotic resistance

1090   genes in global lakes: A review and meta-analysis. Environment International **116**: 60–73.

1091   doi:10.1016/j.envint.2018.04.011

1092   Yang, Y.-Y., G. S. Toor, P. C. Wilson, and C. F. Williams. 2016. Septic systems as hot-spots of

1093   pollutants in the environment: Fate and mass balance of micropollutants in septic drainfields.

1094   Science of The Total Environment **566–567**: 1535–1544. doi:10.1016/j.scitotenv.2016.06.043

1095   York, J. K., G. Tomasky, I. Valiela, and D. J. Repeta. 2007. Stable isotopic detection of ammonium and

1096   nitrate assimilation by phytoplankton in the Waquoit Bay estuarine system. Limnology and

1097   Oceanography **52**: 144–155. doi:10.4319/lo.2007.52.1.0144

1098   Yoshida, T., T. Sekino, M. Genkai-Kato, and others. 2003. Seasonal dynamics of primary production in

1099   the pelagic zone of southern Lake Baikal. Limnology **4**: 53–62. doi:10.1007/s10201-002-0089-3

1100   Yoshii, K. 1999. Stable isotope analyses of benthic organisms in Lake Baikal. Hydrobiologia **411**: 145–

1101   159.

1102   2016a. Methods for determination of nitrogen-containing matters (with corrections) (Методы

1103   определения азотсодержащих веществ (с Поправками)).

1104   2016b. Methods for determination of phosphorus-containing matters (with corrections) (Методы

1105   определения фосфорсодержащих веществ).

1106   2017. Nitrate concentration in waters: Photometric methods with Giress reagent following stabilization in

1107   a cadmium reducer (Массовая концентрация нитратного азота в водах: Методика измерений

1108   фотометрическим методом с реактивом Грисса после восстановления в камиевом

1109   редукторе).

1110

Conflicts of Interest

The authors declare no conflicts of interest.

Table 1: Location, depth, temperature and population information for each of the 17 sampling stations. "OS" refers to pelagic locations (i.e., "Offshore"), whereas other site abbreviations refer to littoral sampling locations.

Site	Latitude	Longitude	Depth (m)	Distance to shore (m)	Air Temperature (°C)	Surface Temperature (°C)	Adjacent Population
BK-1	51.90316	105.07404	0.7	10	18	14	80
BK-2	51.90365	105.069	0.9	17.5	19	13	80
BK-3	51.90536	105.0957	0.8	10	18	14	80
BGO-1	52.02693	105.40102	0.9	18	20	13	0
BGO-2	52.0197	105.37707	1.1	14	19	14	600
BGO-3	52.02649	105.43577	0.7	21	18	16	600
OS-1	51.98559	105.47237	900	NA	15	NA	NA
KD-1	51.92646	105.24504	0.8	20.75	23	NA	0
KD-2	51.91807	105.21456	0.9	14.5	23	16	0
MS-1	51.89863	105.15017	0.6	10.5	21	17	0
SM-1	51.87152	104.98006	0.9	11.5	21	15	0
LI-1	51.86825	104.83042	0.6	8.9	19	14	2000

LI-2	51.84626	104.87356	0.8	9.4	21	15	2000
LI-3	51.85407	104.86216	0.7	9.25	19.5	15	2000
EM-1	51.86005	104.93999	0.7	15.5	24.5	14	0
OS-2	51.8553	104.8148	1300	NA	21	NA	NA
OS-3	51.859108	105.0769	1400	5000	NA	14.5	NA

1130
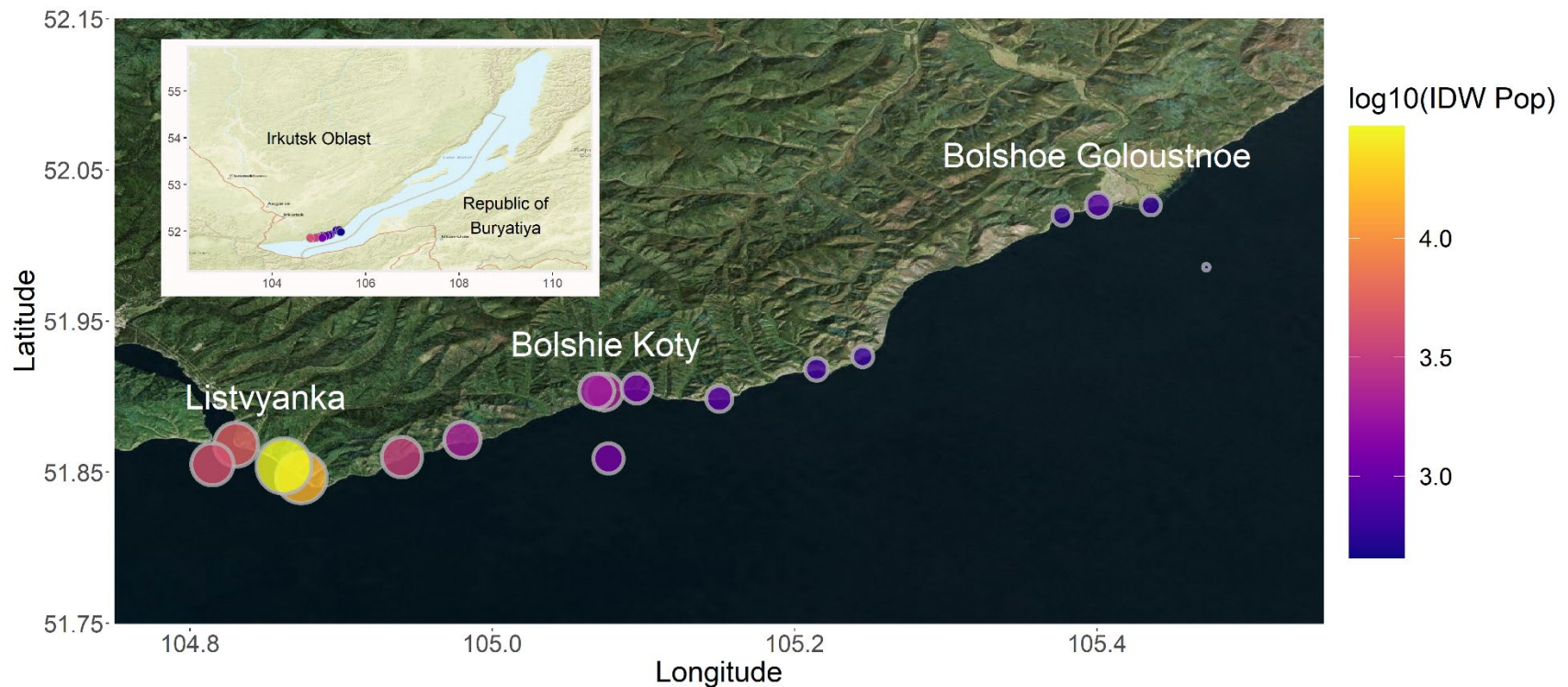
1131

1132 Figure 1: Map of all sampling locations with sites sized and colored by log-transformed IDW population. IDW population was log-

1133 transformed so as to make IDW populations across three orders of magnitude more comparable. The entire transect included three

1134 developed sites (i.e., Listvyanka, Bolshie Koty, Bolshoe Goloustnoe). Three offshore samples were also collected to compare pelagic

1135 sewage signals to those in the littoral. Sampling locations west of Listvyanka are located farther from Listvyanka's centroid, and

1136 therefore have lower IDW population values than sites located closer to the centroid. This map was created using the R statistical

1137   environment (R Core Team 2019) and the tidyverse (Wickham et al. 2019), OpenStreeetMap (Fellows and Stotz 2019), ggpubr

1138   (Kassambara 2019), cowplot (Wilke 2019), and ggrepel (Slowikowski 2019) packages.

1139

1140

Bolshoe Goloustnoe (600 pop.)

Bolshie Koty (80 pop.)

Listvyanka (1,963 pop.)
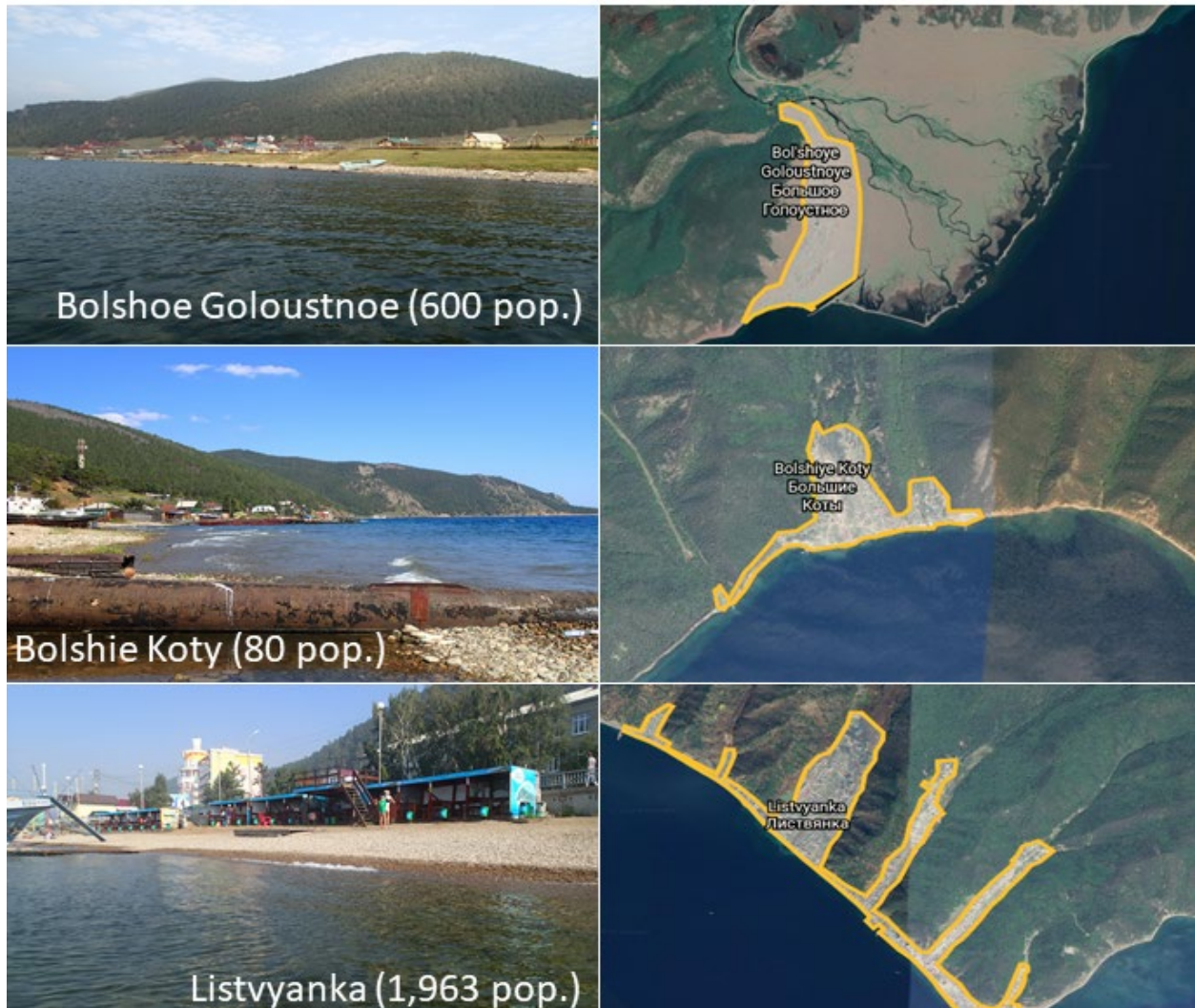
1141

1142 Figure 2: Photographs and Google Earth imagery of each developed area. Photographs were

1143 taken by Kara H. Woo and Michael F. Meyer.

Table 2: Average sewage indicator concentrations and densities per sampling location. Caffeine, acetaminophen/paracetamol, paraxanthine, and cotinine detection limits are estimated to be 0.001 µg/L based on a 500 mL sample volume.

| Site	NH$_4^+$ (mg/L)	NO$_3^-$ (mg/L)	Total Phosphorus (mg/L)	Caffeine (µg/L)	Acetaminophen (µg/L)	Paraxanthine (µg/L)	Cotinine (µg/L)	Fragment density (MPs/L)	Fiber density (MPs/L)	Bead density (MPs/L)	IDW population	Categorical IDW population
BK-1	0.003	0.085	0.054	0.011	0.001	0.002	0	0	0.000833	0	2304.039	High
BK-2	0.003	0.085	0.052	0.007	0.001	0	0	0.000952	0.000476	0	1891.558	Mod/Low
BK-3	0.068	0.09	0.045	0.003	0.001	0	0	0.003095	0.00119	0	1231.234	Mod/Low
BGO-1	0.0145	0.085	0.044	0	0.002	0	0	0.00119	0	0	838.5385	Mod/Low
BGO-2	0.001	0.08	0.0385	0	0.001	0	0	0.000238	0.001905	0	611.91	Mod/Low
BGO-3	0.001	0.09	0.044	0.005	0.003	0	0	0	0	0	624.455	Mod/Low
OS-1	0.001	0.085	0.061	0	0.001	0	0.001	0.002381	0	0	455.7733	Mod/Low
KD-1	0.0035	0.065	0.0375	0.003	0.001	0	0	0	0.000476	0	662.4151	Mod/Low
KD-2	0.001	0.1	0.0445	0.001	0.001	0	0	0.000714	0.001905	0	720.5484	Mod/Low
MS-1	0.001	0.09	0.061	0.064	0.035	0.015	0	0	0.000238	0	903.6733	Mod/Low
SM-1	0.001	0.085	0.1475	0.042	0.012	0.005	0	0	0.001667	0	2146.218	Mod/Low
LI-1	0.004	0.08	0.0385	0.05	0.04	0.006	0.002	0.00381	0.000238	0.000714	5403.209	High
LI-2	0.091	0.095	0.0775	0.001	0.007	0	0	0.001429	0.00119	0	14792.51	High
LI-3	0.0035	0.08	0.077	0.027	0.002	0.002	0.003	0.000476	0	0.000714	29511.73	High
EM-1	0.1125	0.185	0.092	0.029	0.014	0.002	0	0	0.000238	0	3389.949	High
OS-2	0.001	0.08	0.078	0.033	0.001	0.004	0.003	0.000238	0.001905	0	4340	High
OS-3	0.001	0.08	0.0795	0.001	0.001	0	0	0	0.002143	0	1221.424	Mod/Low

1144

A PPCP vs. IDW Population
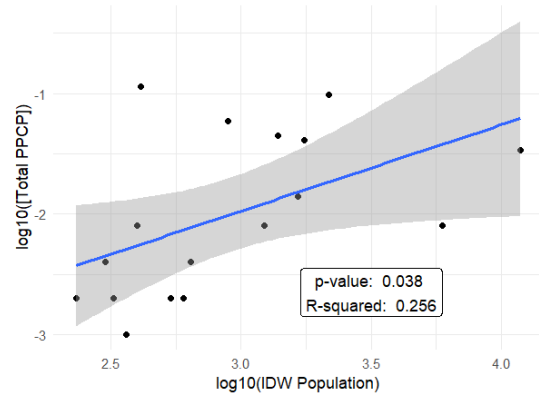
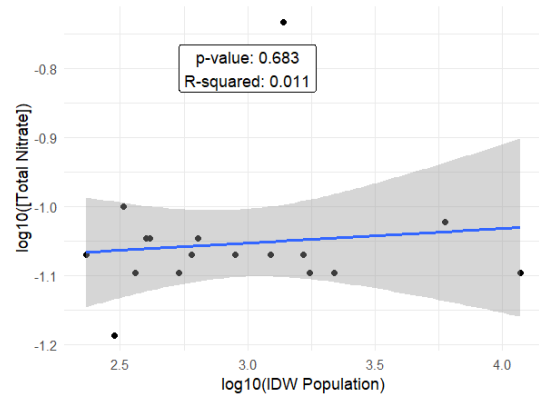**B** δ^{15}N ‰ vs. IDW Population
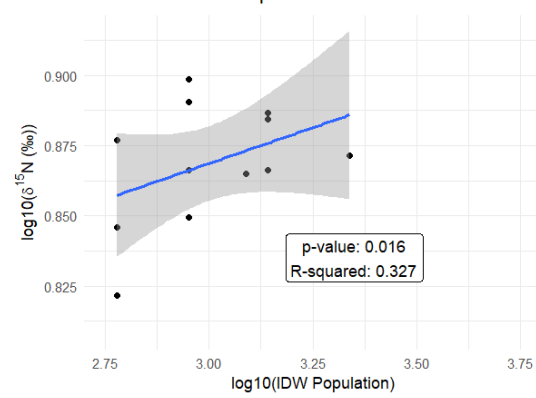
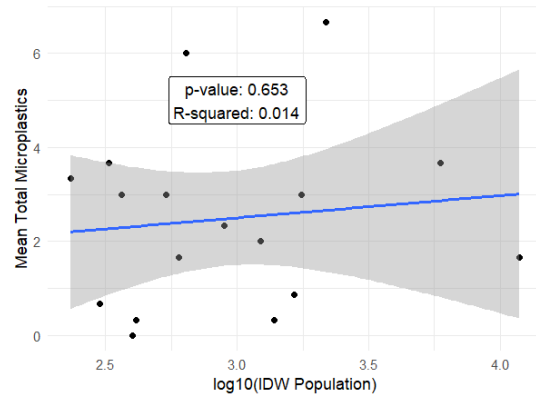**C** Phosphorus vs. IDW Population
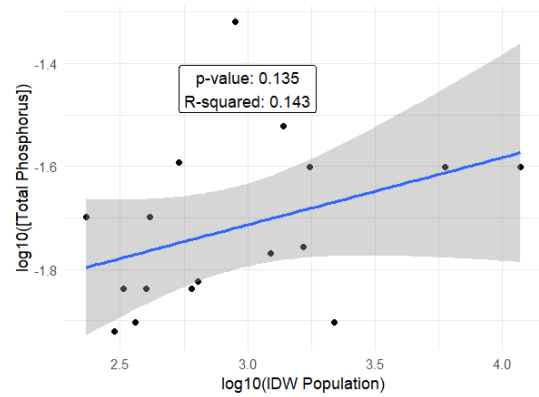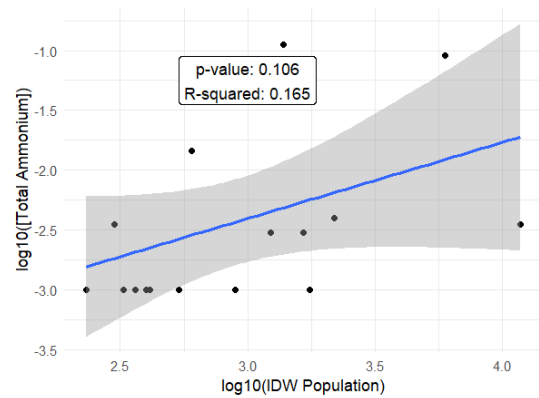
D Chlorophyll a vs. IDW Population
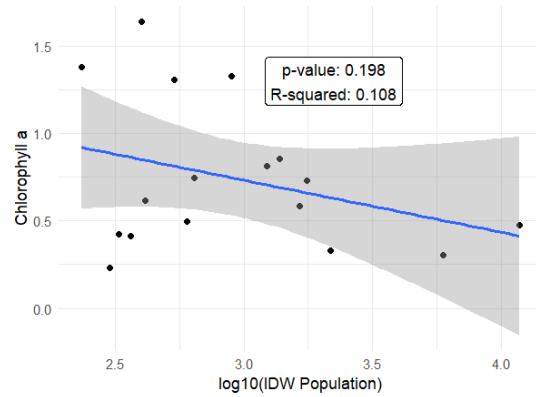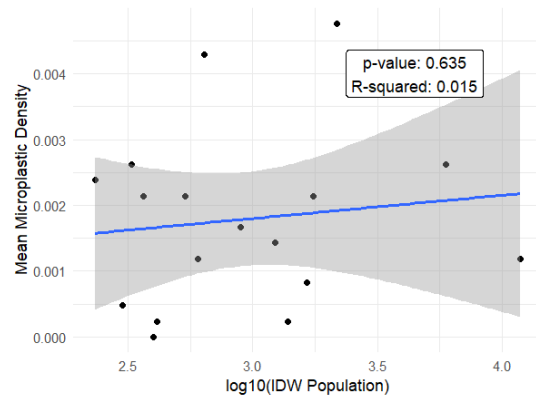
E Nitrate vs. IDW Population

**F** Total Microplastics vs. IDW Population

G Ammonium vs. IDW Population

H Microplastics Density vs. IDW Population

1145

1146 Figure 3: Linear models of total PPCP concentrations (A), macroinvertebrate $\delta^{15}N$ (B), total

1147 phosphorus (C), chlorophyll a (D), nitrate (E), total microplastics (F), ammonium (G), and

1148 microplastic density (H) regressed against log-transformed inverse distance weighted (IDW)

1149 population. Total PPCP concentrations (A) and macroinvertebrate $\delta^{15}N$ (B) produced significant

1150 models. Total phosphorus (C), chlorophyll a (D), nitrate (E), total microplastics (F), ammonium

1151 (G), and microplastic density (H) did not produce significant models.
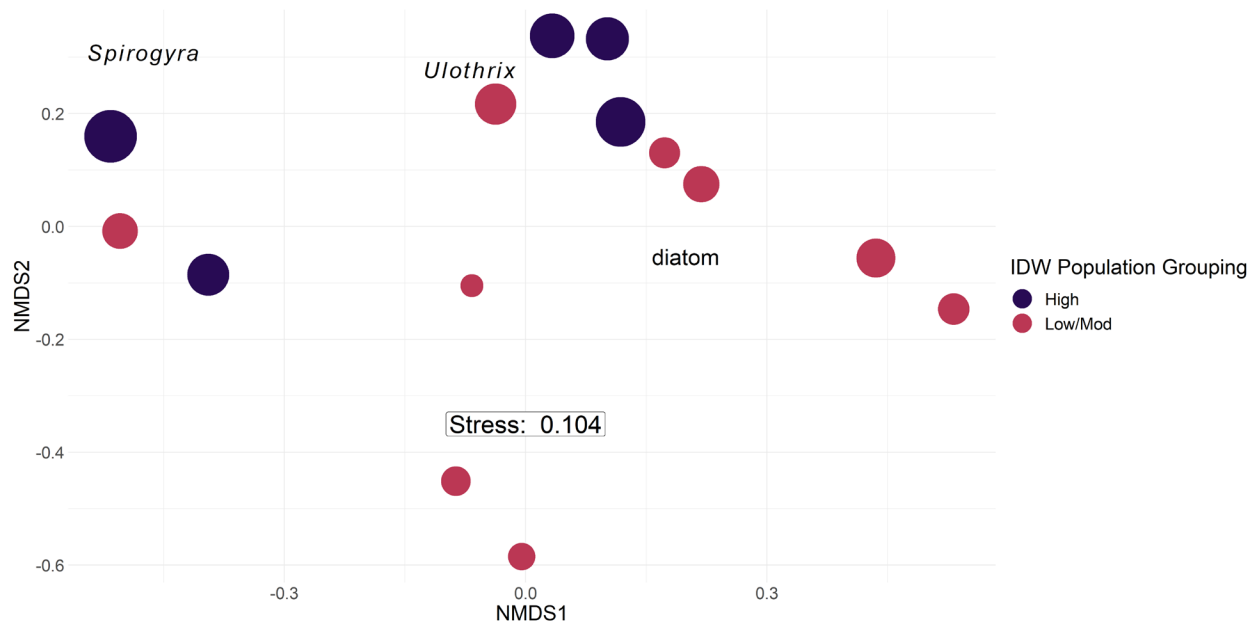
1152

Figure 4: Periphyton abundance NMDS with Bray-Curtis dissimilarity. Points are sized by log10

IDW population and colored by grouped IDW population values. Taxonomic labels represent

species scores, which are weighted averages of species contributions from site scores. For

periphyton, PERMANOVA (p = 0.001) and post-hoc SIMPER results suggested sites with a

higher IDW population value tended to be more associated with filamentous algal groupings and

separate from sites with moderate and low IDW population values, which were more associated
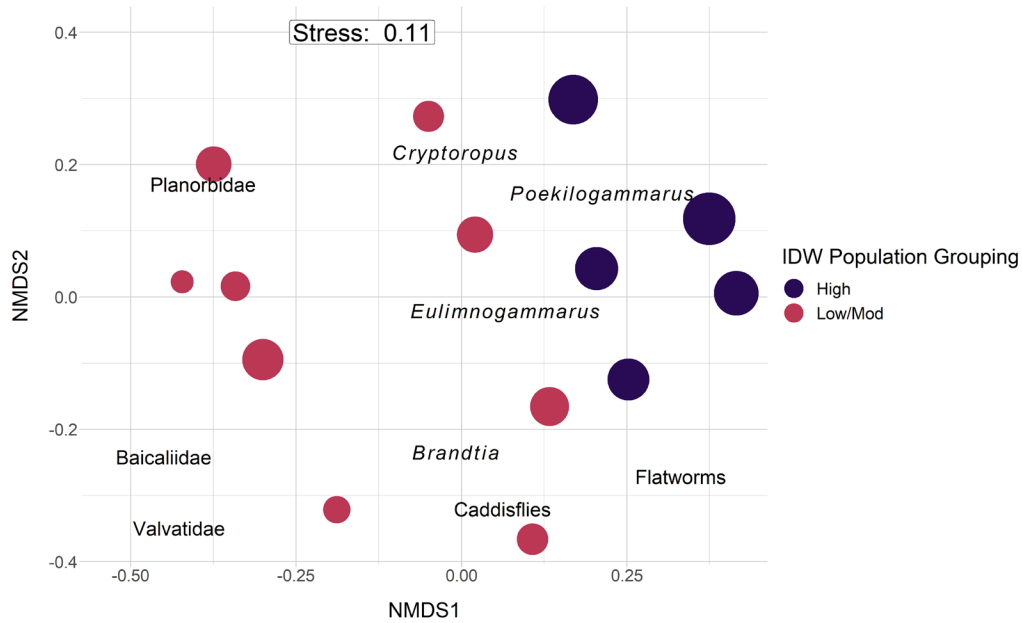
with diatom abundance.

1160

Figure 5: Macroinvertebrate abundance NMDS with Bray-Curtis dissimilarity. Points are sized by log10 IDW population and colored by grouped IDW population values. Taxonomic labels represent species scores, which are weighted averages of species contributions from site scores. For macroinvertebrates, PERMANOVA (p = 0.02) and post-hoc SIMPER results suggested sites with a higher IDW population values tended to be associated with amphipod taxa (see Table S1), whereas sites with lower and moderate IDW population values were more associated with increased mollusk abundance (see Table S1).
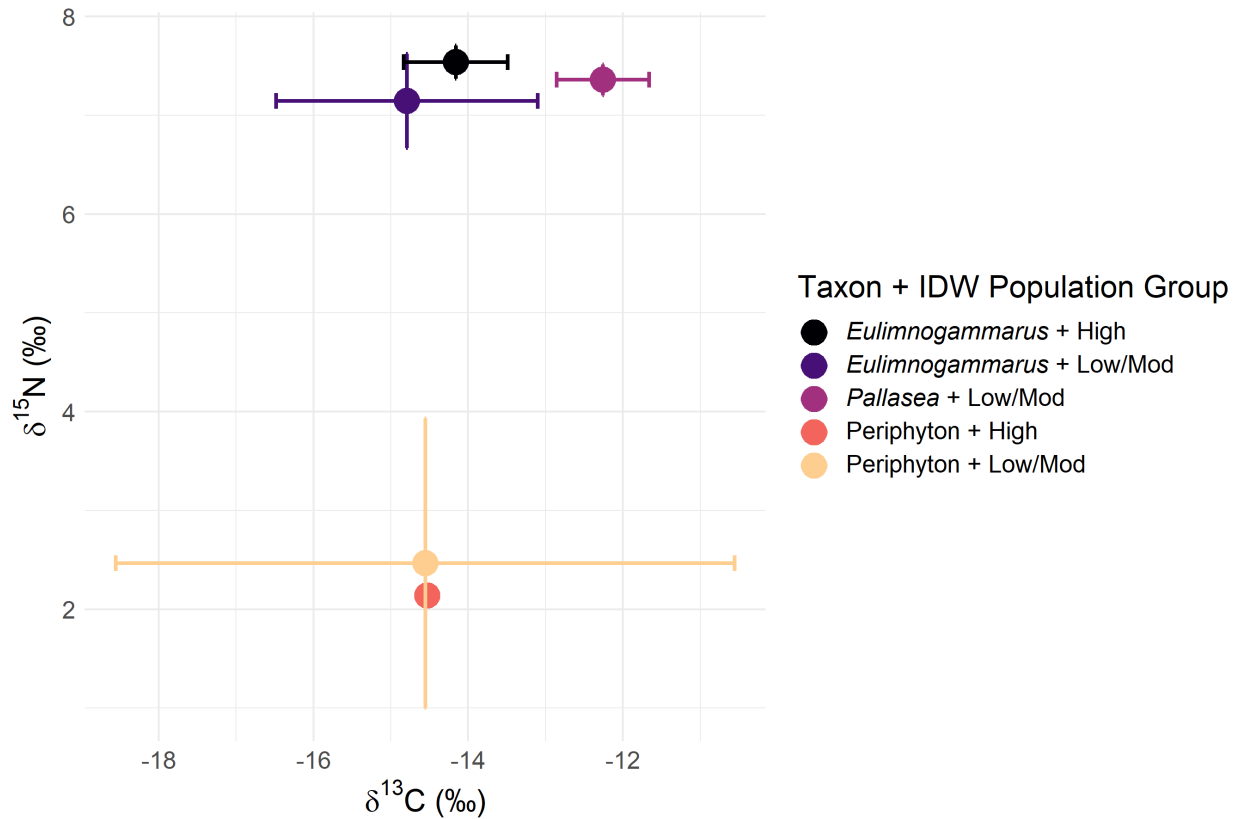
1170

1171

1172   Figure 6: Biplot of mean and standard deviation $\delta^{13}C$ and $\delta^{15}N$ stable isotope values for littoral

1173   amphipods and periphyton, grouped by categorical IDW population (Table 2). In general,

1174   periphyton did not differ in $\delta^{13}C$ or $\delta^{15}N$ signatures with increasing IDW population, whereas

1175   *Eulimnogammarus* amphipods increased in $\delta^{15}N$ signatures with increasing IDW population.

1176   *Pallasea* signatures differed from *Eulimnogammarus* most likely because *Pallasea* tends to

1177   remain in the nearshore area, whereas *Eulimnogammarus* will regularly migrate to deeper zones

1178   (Takhteev & Didorenko, 2015).

1179

Table 3: Mean inter-site fatty acid proportion of each taxon and fatty acid grouping (as defined in Table S2).

| Taxon	Number of sites	Branched	LCPUFA	MUFA	SAFA	SCPUFA
Draparnaldia spp.	4	0.000	0.012	0.088	0.189	0.710
Eulimnogammarus cyaneus	2	0.002	0.259	0.309	0.248	0.182
Eulimnogammarus verrucosus	6	0.000	0.188	0.385	0.240	0.187
Eulimnogammarus vittatus	6	0.001	0.171	0.371	0.241	0.216
Pallasea cancellus	3	0.001	0.282	0.359	0.187	0.171
Periphyton	7	0.000	0.073	0.092	0.284	0.550
Snail	3	0.002	0.470	0.123	0.194	0.211

1180

1181

1182
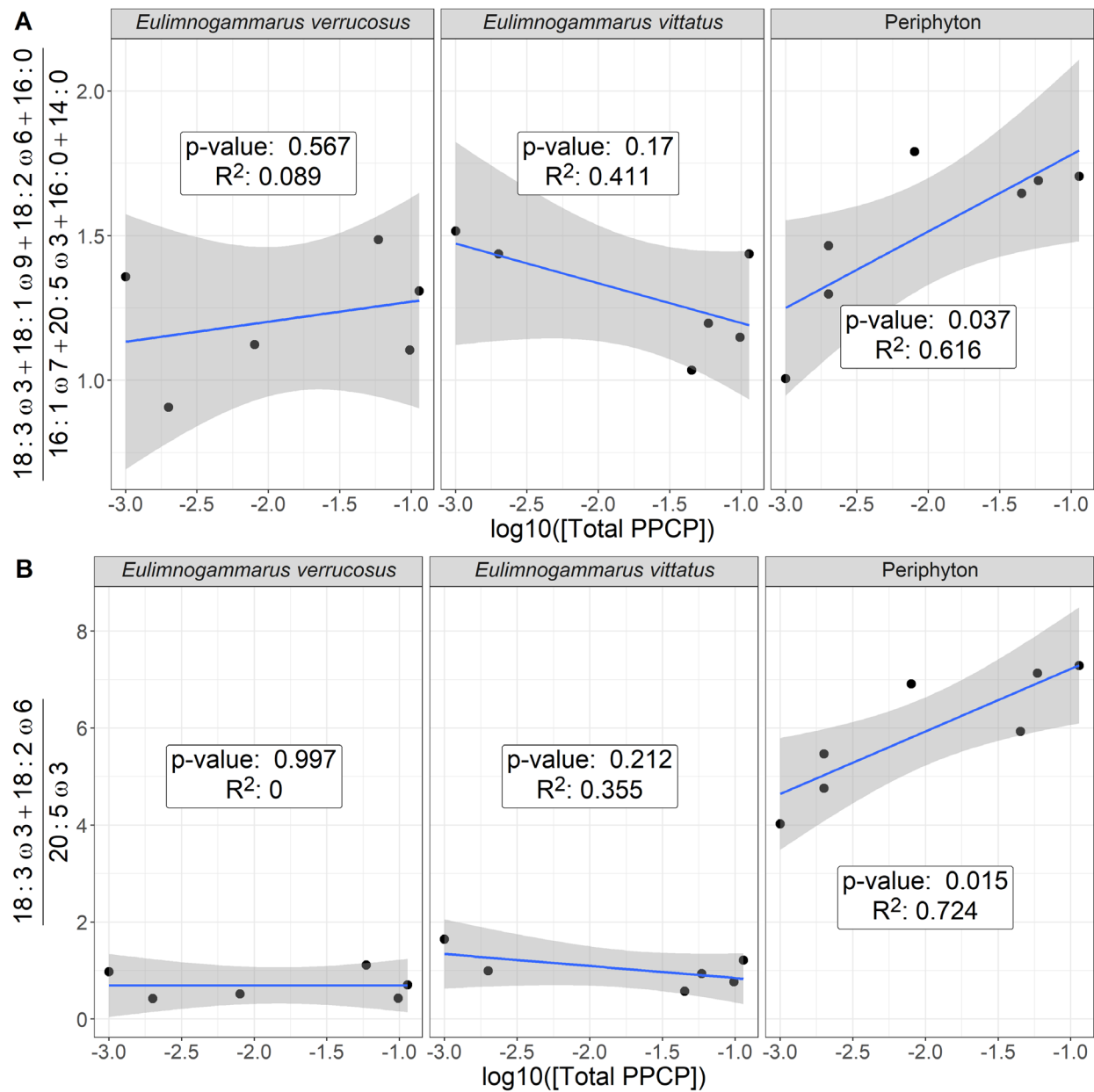
Figure 7: Ratio of filamentous:diatom-associated fatty acids (A) and essential fatty acids (B)

across our PPCP gradient. Our first analysis (A) focused solely on green filamentous algal fatty

acids (i.e., 18:3ω3, 18:1ω9, 18:2ω6, and 16:0 relative to diatom fatty acids (i.e., 20:5ω3, 16:1ω7,

16:0, 14:0) in relation to increasing PPCP concentrations. This first analysis suggested

periphyton reflected an increasing green, filamentous signature relative to diatoms, which

1188   corroborates analyses showing community compositional shifts (Figure 4). While periphyton

1189   fatty acids changed significantly across our sewage gradient, macroinvertebrate signatures

1190   remained consistent. Our second analysis (B) focused solely on the essential fatty acids, which

1191   further highlights the trends observed in periphyton and macroinvertebrate grazers.